

## **Reply to reviewers' comments on "Oceanic and Atmospheric forcing of Larsen C Ice Shelf thinning"**

We are very grateful to both referees for their support and constructive reviews, which have been invaluable in clarifying the paper. Their comments are re-printed in blue text below, with responses wherever needed. We note also that we have changed the title of the paper in response to the reviewers' comments. We have uploaded a revised version of the paper with 'tracked changes' highlighted, and the line numbers below refer to lines in this uploaded document.

In addition to responding to these reviewer comments, we have modified the paper in response to three new relevant studies. Jansen et al. (2015) detail the propagation of a large rift in LCIS that may proceed to threaten its compressive arch, Paolo et al. (in press) show that the surface lowering of LCIS has recently focussed on Bawden Ice Rise, and Khazendar et al. (in press) show that the remnant Larsen B Ice Shelf is showing clear signs of instability.

### **Anonymous Referee #1**

#### **General**

This paper sets out to resolve a long-standing issue on the causes of Larsen C ice shelf thinning. While earlier studies ascribe the surface lowering/thinning to enhanced basal ice melt, later studies suggested that firn compaction, notably its northern regions, could also have a major impact. By quantifying both terms separately along a survey line in the central ice shelf area, that has been revisited multiple times, the authors conclude that it is likely that both processes explain a similar amount of surface lowering along this line. However, the uncertainties remain large because of the heterogeneous datasets used, which contain significant noise. The extensive error analysis does justice to these uncertainties and provides the right context to interpret the results.

#### **Recommendation**

The paper is well and clearly written, albeit somewhat long, and the figures are of good quality. It is certainly an original and important contribution to an important research topic, and the science, including an extensive uncertainty estimate, appears careful and robust. That is why my assessment is that relatively minor revisions are needed for this paper to become publishable in *The Cryosphere*, see below.

#### **General comments**

In the introduction, previous studies on the possible reasons for the surface lowering of LCIS are discussed, but no introductory discussion is dedicated to the spatial variability in observed elevation changes (Figs. 1a and 1b). In previous studies, were these significant variations thought to represent measurement uncertainty or real signals, or both? Please elaborate.

The spatial variations since 1994 are regarded as a real signal in all studies. Some have used the northward intensification of lowering as evidence of a surface melting influence, since surface melting is known to be strongly northward-intensified. This argument is only indicative, however, because we have little knowledge of the spatial distribution of ocean

melting. We have strengthened the sentence announcing the variation (line 55) and draw the reviewer's attention to the sentence outlining the melting argument (line 99).

In spite of (or owing to!) the careful consideration of all potential sources of error, the uncertainties in the final results are large, and that is why I feel the title could be somewhat less 'definitive', for instance by starting with the wording 'A primary estimate of...', as is used in the first sentence of the discussion.

We considered this at some length, but couldn't come up with a better title that succinctly captures the focus of the study. We feel that something like 'An assessment of oceanic and atmospheric forcing of Larsen C Ice Shelf thinning' contains too many sub-clauses. The abstract faithfully describes that we are assessing these forcings, and that our reported results are a primary estimate subject to considerable uncertainties. In the title, we have swapped 'Atmospheric and oceanic forcing...' to 'Oceanic and atmospheric forcing...' to reflect our primary finding of a greater role for ice loss than air loss (see response to reviewer 2).

p. 256, l. 8: Can the presence of liquid water really be ruled out, given the recent finding of perennial firn aquifers in Greenland?

Boreholes drilled in LCIS have yielded no evidence of a perennial aquifer. Specifically, 6 holes drilled by hot water and instrumented with thermistors in 3 widely dispersed locations produced no evidence of a borehole pressure drop, reduced drilling progress, or thermal signature that would be expected from an aquifer (personal communications with Keith Nicholls and Bryn Hubbard, 2015). The sentence has been modified to state that there is no evidence for a perennial aquifer (line 144), and this is now fully described in section 4.3 (line 568).

p. 260: Can the assumption that the southward decrease in surface elevation between surveys, which in the paper is now simply ascribed to increasing radar penetration to the south, where firn air content increases, be corroborated for instance by a quantitative comparison with firn air content (e.g. using the data of Holland and others, 2011)?

A quantitative comparison is not justified because radar penetration is affected only by the top few metres of firn, while the study of Holland et al. (2011) derives the total column-integrated firn air content, and there are many reasons why the two might not co-vary in detail. Nevertheless, we feel it is worthwhile noting that the southward decrease in elevation difference is at least consistent with less compact firn (greater penetration) in the south. The sentence has been modified to emphasise the qualitative nature of this agreement. (line 299).

Fig. 4: Why are no data points provided for ice and air thickness anomalies and the satellite data?

The satellite data are a timeseries of quasi-monthly data from the 5 merged crossovers (section 2.5), and to add them to the plot would make it extremely dense. We never derive ice and air thickness anomalies for the individual surveys; equations (5) and (6) show how ice and air trends are derived directly from elevation and TWTT trends (i.e. the blue and black dashed lines in Figure 4 are derived directly from the green and red dashed lines). This has the advantage that uncertain quantities that are steady in time, such as the geoid and mean dynamic topography, are explicitly excluded from the calculation. This is now fully explained (line 178).

p. 264, l. 21: Replacing the surveyed elevation trend with the satellite elevation trend (Fig. 5a vs. Fig. 7a) completely changes the interpretation of the air loss signal, from one that is monotonically increasing in magnitude from north to south, to one that has a maximum magnitude in center of the survey line. In view of this rather arbitrary swapping of data, the word 'conclude' (p. 264, l. 26) is too strong to my taste, and should be replaced by something like 'hypothesise'.

Changed to 'Figure 7a suggests that...' (line 419).

#### Specific comments

p. 252, l. 11: "Though the ice loss is much larger, ice and air loss contribute approximately equally to the lowering." This is ambiguous; the word 'larger' has no explicit meaning here (mass, vertical motion?). Please reformulate in terms of contributions to ice shelf thinning or surface lowering.

The preceding sentence says that the lowering is caused by ice loss of  $\sim 0.3$  m/y and air loss of  $\sim 0.03$  m/y. The ice loss is larger. We have changed the sentence to 'The ice loss is much larger than the air loss, but both contribute approximately equally to the lowering because the ice is floating' (line 22).

p. 253, l. 7: Please explain how firn compaction could -indirectly- have led to ice shelf weakening.

Changed to 'However, longer-term processes such as ice thinning and firn compaction must first have driven these ice shelves into a state liable to collapse by weakening the ice and enabling meltwater to pool on the ice surface' (line 49).

p. 254, l. 21: and THAT the northern edge of LCIS is at this limit...(?)

Changed to '... suggests that atmospheric warming may have pushed some ice shelves beyond a thermal limit of viability (Morris and Vaughan, 2003); the northern edge of LCIS is at this limit' (line 96).

p. 254, l. 23: high -> significant.

Changed to 'higher' (line 98).

p. 254, l. 26: Modelled firn compaction entirely offset the lowering in one study of 2003–2008 (Pritchard et al., 2012), BUT WITH A LARGE UNCERTAINTY

Changed to 'albeit with a high uncertainty' (line 102).

p. 255, l. 3: suggest to remove 'strongly'

The trends are strongly negative and so we prefer the sentence as it is (line 106).

p. 257: In expressions 7 and 8, is the different in significant numbers in the factors real, or should 1.06 be 1.060?

All numbers are given with 3 significant figures; there is no difference (line 184).

p. 259, l. 24: thinner -> smaller

Changed to 'lower' (line 260).

p. 261, l. 24: "... that is not supported by the remaining data." What remaining data?

Changed to 'This is important because studies of LCIS that include these early data (Fricker and Padman, 2012; Shepherd et al., 2003) derive very rapid lowering in the 1990s that is not found if the early data are neglected' (line 328).

p. 263, l. 19: If anomalies relative to 2004 are presented, should then 2004 not have a zero point for elevation, or are these hidden behind the red dot? Why no uncertainty for that point?

The dot for 2004 elevation anomalies relative to 2004 is indeed hidden behind the TWTT anomaly dot, since both are zero. The 2004 data have no error because the error bars refer to the standard error of the differences between the individual data points in each survey and their 2004 counterparts. Both points are now clarified in the text and figure caption. (lines 385 and 1157).

p. 294, Fig. 5a: the blue point in the legend appears to be a point in the graph, consider moving the legend to upper part of graph.

We have enclosed the legends for figures 5a and 7a in boxes.

## Review comments by A. Khazendar

### Overview

The main objective of the manuscript is to describe a technique that partitions observed ice-shelf surface elevation changes into components of ice and air content changes. The technique combines measurements of surface elevation changes with contemporaneous travel times through the ice shelf of a radar signal. The method is applied to 8 surveys of a transect in the central part of the Larsen C Ice Shelf. The authors conclude that the observed surface lowering was probably due to both air and ice loss, with air loss more likely to be the more prevalent of the two. Possible implications of these findings for the stability of Larsen C are then discussed.

We are concerned that the reviewer has concluded that air loss is more likely to be the prevalent cause of the lowering. Our primary estimate is that ice loss is an order of magnitude larger than air loss and so we would argue that ice loss is the dominant change implied by our results. This is a complex issue, however, for two reasons: 1) since the ice is floating, these rates of ice loss and air loss contribute approximately equally to the lowering (within error bars they have the same effect on lowering, though the central estimate is that the air loss has a slightly larger effect); 2) if one arbitrarily neglects individual surveys, it is possible to render insignificant the conclusion of ice loss, but the conclusion of air loss is robust (Table 2).

We have addressed this issue by re-ordering the title to ‘Oceanic and atmospheric forcing...’ rather than ‘Atmospheric and oceanic forcing...’, emphasising in the abstract that the ice loss is much larger than the air loss (line 22), and emphasising in the conclusions that we argue ice loss to be the dominant change affecting LCIS (line 864).

The work addresses an important question. Attributing observed thinning in peninsular ice shelves to oceanic or atmospheric causes has been long debated as part of the effort to understand the destabilization of these ice shelves. Ice shelves on the eastern peninsula generally have lower basal melting rates compared with elsewhere in Antarctica, hence atmospheric warming could be as important a factor in observed ice shelf thinning as enhanced basal melting, if not more so.

The method devised is highly innovative and promising. One of the main challenges in implementing it is the high uncertainty of the observations, especially in a situation where observed thinning rates are relatively low. The authors address this issue with an extensive discussion of the errors involved and by using different combinations of the data sets in performing their calculations. The manuscript could probably benefit from review by someone with more knowledge of statistical error analysis than I do. Apart from the uncertainties, one aspect of the theory remains unclear as discussed below.

See response below.

The manuscript is mostly very well written and presented, if somewhat sprawling. In particular, parts of section 5.2 on ice-shelf stability read like a review paper with little relevance to the current work and can benefit from some abridgement.

Section 5.2 reviews the future prognosis for LCIS. Since our results allow us to assess ice-loss and air-loss timescales for the first time, it was not previously possible to speculate with any

certainty upon the possible mechanisms for imminent LCIS collapse. We regard this as a crucial exposition of the implications of this work, which is all the more important in light of the Jansen et al. (2015), Paolo et al. (in press), and (Khazendar et al., in press) papers and the possibility that LCIS collapse is now imminent. We have shortened section 5.2 wherever possible.

### Main remarks

P. 256, equations 1 and 2: neither equation has information about the relative vertical distributions of ice and air in the ice shelf. The method as I understand it would work, however, because it combines the observed surface elevation with the observed change in TWTT. The combination constrains the possible partitioning scenarios and is able to attribute the observed change to ice and/or air change. This approach, however, seems to have an underlying assumption. Namely, that signal propagation in, and the dielectric properties of, an ice/air mixed medium will change linearly with the change of ratio of air to ice. Is this the case?

Equation (2) states that the total delay of the radar wave passing through the ice shelf is the linear sum of the delay due to the total solid ice thickness and the delay due to the total thickness of air inclusions in the firn. This is also known as the ‘Complex Refractive Index Method’ and has been used in quite a few studies of glaciological radar data. The method is introduced briefly and equation (2) is now provided with a reference to the CRIM (Arcone, 2002) (line 157).

P. 268 L. 5: I believe that instrument and processing specifications and errors deserve more discussion, especially given the relatively small thinning rates in this study. For example, what is the time resolution and bandwidths of the instruments used, and are they sufficient to distinguish unambiguously the changes in TWTT?

This is an extremely good question, to which the answer is complex. In the text below, we use ‘precision’ to refer to the length of time between samples of the radar return echo power. We understand the reviewer’s question to be whether or not the precision in the data is fine enough to capture the observed thinning signal.

The TWTT data are recorded with a wide variety of instruments and subject to different processing techniques to optimise the signal prior to picking (Table 1 and Section 2.3). When considering the TWTT changes, the important measure is not the precision of the instrument, it is the precision of the processed data from which the TWTT is picked. This is usually lower than that of the instrument, since processing to reduce the noise in the data also reduces the resolution. The precision in the echograms picked varies between surveys, with a mean of ~4 m ice thickness equivalent (~24 nanoseconds) and a range of 0.125–8.8 m ice equivalent. The mean TWTT trend is ~3.5 m ice equivalent over 15 years (Figure 4), and so at face value this trend may seem indistinguishable by the data. There are many factors to be taken into consideration, but there are two primary reasons why this is not the case.

Firstly, the position of the ‘first break’ in the return echoes can be estimated at a higher precision than the TWTT data. The waveform of the echoes are at least 10 times the length of the TWTT precision, and it is the position of a gradient at the leading edge of this waveform that we seek to determine. In our processing, the leading edge is fitted using high-order

interpolation, and the position of the first break is determined at a nominal precision one tenth that of the original data (i.e. a mean of  $\sim 0.4$  m).

Secondly, and most importantly, each difference plotted in Figure 4, from which ice and air trends are calculated, is actually the mean of a population of thousands of point differences, with standard deviations of  $\sim 10$  m (Table 3) and ranges of  $\pm 40$  m (Figure 2). These populations are well-resolved by the TWTT precision, and so we are able to detect the mean difference statistically to a precision much finer than that of the individual data. As an extremely crude illustration, imagine if precision is 1 m ice-equivalent in two surveys and we have observed 1000 TWTT differences between them; if 300 points show a first-break 1 m shorter and 700 show no change, the mean change estimated would be a reduction of 0.3 m; this is less than the 1 m precision of an individual data point but a validly precise estimate of the mean difference between surveys.

We have responded to this point by adding an abridged version of the above discussion to section 2.3 (line 245).

P. 264 L. 19-24: the radar elevation trends were considered unreliable and replaced with satellite elevation trends. I assume that the same TWTT were then used in the calculation of ice and air losses. But, if the radar surface elevations were judged unreliable, wouldn't that mean that the corresponding TWTT should also be considered suspicious, given that TWTT are obtained from the signal travel time between the (unreliable) surface and bottom of the ice shelf?

For airborne surveys, the TWTT and elevation data are independent datasets derived from separate instruments. TWTT through the ice is derived from picking and then differencing the surface and basal echoes from an ice-sounding radar, while elevation is derived separately from an altimeter. The surface pick from the ice-sounding radar is not coincident with the altimeter elevation, and we are free to discard one set of measurements and retain the other, if justified.

In the text referred to, we consider the satellite-derived elevations to be more reliable than the surveyed elevations due to a concern over radar altimeter penetration in the 1998 survey. This could affect the surveyed elevation trend because later surveys use laser altimeters or GPS, which have no surface penetration. That concern does not apply to the TWTT, since the surface pick of the ice-penetrating radars has similar penetration in all surveys. This is now noted (line 412).

Figure 3 and caption: I find these confusing. North of latitude  $-67.8$ , the differences plotted in the figure are positive, implying that the (lower due to penetration) values from 2011 BAS survey were subtracted from the (higher) 2010 IceBridge laser altimetry measurements. South of  $-67.8$ , the caption explains, the 2011 data become progressively lower due to increased radar penetration of the firn, which means that their difference from the 2010 data laser altimetry data should increase, yet the opposite is shown in the figure.

As described in section 2.4, the 2011 radar altimeter elevation data are subject to two problems; first, they require general calibration, and second, they are subject to firn penetration in the south that needs to be removed to make them comparable to the laser altimeters and GPS used in the other surveys.

The differences shown in Figure 3 are 2011 minus 2010. For the uncorrected 2011 data (blue dots) this is generally positive, implying that the 2011 radar altimeter is apparently recording the surface higher than the 2010 laser altimeter, which sampled the surface only 10 weeks earlier and was precisely calibrated. Therefore, we regard this difference as a calibration error and correct the 2011 data by subtracting from them everywhere the mean offset north of 67.85S, 1.59 metres.

After this correction, the blue dots would be shifted downwards by 1.59 metres everywhere. This then produces a negative 2011-2010 difference in the south of the section, i.e. the 2011 radar altimeter is recording the surface lower than the 2010 laser altimeter. We attribute this to radar firn penetration, and correct it by adding a linear fit to the mismatch south of 67.85S. The corrected 2011 data minus the 2010 data are shown by the green dots.

To address this point, we have substantially rewritten the relevant text (line 289 onwards) and also rewritten the figure caption to reflect the above logic.

P. 268 L. 7-8: How does a spatial offset from the reference line introduce an error? Doesn't each data point come with its own spatial coordinate?

LCIS gets progressively thinner from west to east, with a progressively greater firn air content. If one survey were systematically to the west of the others it would sample thicker ice with less air, and this would appear as a temporal change in ice and air; an inter-survey error. Since none of the surveys is systematically offset this is not a problem, but the measurements do not precisely follow the same line, weaving slightly to the east and west, and this introduces intra-survey error. The sentence has been modified to clarify this (line 513).

#### Other remarks

P. 253 L. 6: here or elsewhere in the manuscript, please consider citing earlier work that investigated meltwater-induced ice fracture (e.g., Weertman, 1973; van der Veen, 1998), in addition to the work cited here already.

There is a large body of literature on meltwater-induced ice fracture so in the interest of brevity we have only added the van der Veen reference (line 45).

P. 259 L. 27 and Table 1: if the 2009 IceBridge TWTT data were not included, were any other data from this campaign used in the analyses leading to the final conclusions of the work? If no, why keep referring to 8 surveys instead of 7?

The surveyed elevation data from the 2009 IceBridge survey were used throughout, so the paper does consider 8 surveys. The retention of the elevation data from 2009 is now explicitly stated (line 264).

P. 253 L. 25-26: ocean water at or below sea-surface freezing temperature could still melt ice at depth. Replacing "sea-surface" with "in situ" would probably be more accurate.

Changed to '...found the ocean to be at or below the surface freezing temperature, suggesting that it is only capable of slow melting' (line 71).

P. 253 L. 27-29: even if marine ice presence were widespread it does not necessarily mean that cooler ocean temperatures are spatially and temporally prevalent. Existing marine ice could have accumulated mostly under past conditions.

Changed to 'widespread marine ice in LCIS suggests that these temperatures are spatially and historically prevalent' (line 74).

P. 254 L. 5: consider showing the location of the sonar measurements on the map of Fig. 1.

Sentence changed to 'sonar measurements near Kenyon Peninsula in the south of LCIS' (line 79).

P. 252 L. 16: "in [the] future".

We prefer the original wording, which is valid English usage (line 28).

## References

- Arcone, S. A.: Airborne-radar stratigraphy and electrical structure of temperate firn: Bagley Ice Field, Alaska, USA, *Journal of Glaciology*, 48, 317-334, Doi 10.3189/172756502781831412, 2002.
- Holland, P. R., Corr, H. F. J., Pritchard, H. D., Vaughan, D. G., Arthern, R. J., Jenkins, A., and Tedesco, M.: The air content of Larsen Ice Shelf, *Geophysical Research Letters*, 38, L10503, 10.1029/2011gl047245, 2011.
- Jansen, D., Luckman, A. J., Cook, A., Bevan, S., Kulesa, B., Hubbard, B., and Holland, P. R.: Newly developing rift in Larsen C Ice Shelf presents significant risk to stability, *The Cryosphere Discussions*, 9, 861-872, 10.5194/tcd-9-861-2015, 2015.
- Khazendar, A., Borstad, C. P., Scheuchl, B., Rignot, E., and Seroussi, H.: The evolving instability of the remnant Larsen B Ice Shelf and its tributary glaciers, *Earth and Planetary Science Letters*, 10.1016/j.epsl.2015.03.014, in press.
- Paolo, F. S., Fricker, H. A., and Padman, L.: Volume loss from Antarctic ice shelves is accelerating, *Science*, in press.

1 ~~Atmospheric and oceanic~~Oceanic and atmospheric forcing of

2 **Larsen C Ice Shelf thinning**

3 Paul R. Holland<sup>1</sup>, Alex Brisbourne<sup>1</sup>, Hugh F.J. Corr<sup>1</sup>, Daniel McGrath<sup>2,3</sup>, Kyle Purdon<sup>4</sup>, John  
4 Paden<sup>4</sup>, Helen A. Fricker<sup>5</sup>, Fernando S. Paolo<sup>5</sup>, and Andrew Fleming<sup>1</sup>.

5

6 <sup>1</sup>British Antarctic Survey, Cambridge, UK.

7 <sup>2</sup>USGS Alaska Science Center, Anchorage, Alaska, USA.

8 <sup>3</sup>Cooperative Institute for Research in Environmental Sciences, University of Colorado,  
9 Boulder, Colorado, USA

10 <sup>4</sup>Center for Remote Sensing of Ice Sheets, University of Kansas, Lawrence, Kansas, USA.

11 <sup>5</sup>Scripps Institution of Oceanography, University of California, San Diego, La Jolla, California,  
12 USA.

13 **Abstract**

14 The catastrophic collapses of Larsen A and B ice shelves on the eastern Antarctic Peninsula  
15 have caused their tributary glaciers to accelerate, contributing to sea-level rise and freshening  
16 the Antarctic Bottom Water formed nearby. The surface of Larsen C Ice Shelf (LCIS), the  
17 largest ice shelf on the peninsula, is lowering. This could be caused by unbalanced ocean  
18 melting (ice loss) or enhanced firn melting and compaction (englacial air loss). Using a novel  
19 method to analyse eight radar surveys, this study derives separate estimates of ice and air  
20 thickness changes during a 15-year period. The uncertainties are considerable, but the primary  
21 estimate is that the surveyed lowering ( $0.066\pm 0.017$  m/y) is caused by both ice loss ( $0.28\pm 0.18$   
22 m/y) and firn air loss ( $0.037\pm 0.026$  m/y). ~~Though the ice loss is much larger~~ than the air loss,  
23 but ice and air loss both contribute approximately equally to the lowering because the ice is  
24 floating. The ice loss could be explained by high basal melting and/or ice divergence, and the  
25 air loss by low surface accumulation or high surface melting and/or compaction. The primary  
26 estimate therefore requires that at least two forcings caused the surveyed lowering.  
27 Mechanisms are discussed by which LCIS stability could be compromised in future, ~~suggesting~~  
28 ~~destabilisation timescales of a few centuries~~. The most rapid pathways to collapse are offered  
29 by ~~a flow perturbation arising from~~ the ungrounding of LCIS from Bawden Ice Rise, or ice-  
30 front retreat past a 'compressive arch' in strain rates. Recent evidence suggests that either  
31 mechanism could pose an imminent risk.

## 32 1. Introduction

33 The ice shelves of the Antarctic Peninsula (AP) have shown a progressive decline in extent  
34 over the last five decades, including the catastrophic collapses of Larsen A Ice Shelf (LAIS) in  
35 1995 and Larsen B Ice Shelf (LBIS) in 2002 (Scambos et al., 2003; Cook and Vaughan, 2010).  
36 The collapse of LBIS was unprecedented in at least the last 12,000 years (Domack et al., 2005).  
37 These collapses have reduced the restraint of the ice shelves on the flow of grounded tributary  
38 glaciers, causing them to accelerate (Rignot et al., 2004; Berthier et al., 2012) and thereby  
39 contributing to sea-level rise (Shepherd et al., 2012). Increased freshwater input to the ocean  
40 from the collapses and subsequent excess ice discharge ~~is also thought to have freshened~~may  
41 be implicated in the freshening of~~the~~ Antarctic Bottom Water formed nearby (Hellmer et al.,  
42 2011; Jullion et al., 2013).

43

44 These ice-shelf collapses are thought to have been accomplished by surface meltwater-driven  
45 crevassing (van der Veen, 1998; Scambos et al., 2003; van den Broeke, 2005; Banwell et al.,  
46 2013) and ice-front retreat past a ‘compressive arch’ in strain rates (Doake et al., 1998; Kulesa  
47 et al., 2014). ~~The final collapses have been attributed to meltwater induced ice fracture~~  
48 ~~following years of extreme atmospheric melting [Banwell et al., 2013; Scambos et al., 2003;~~  
49 ~~van den Broeke, 2005]~~However, but longer-term, longer-term processes such as ice thinning  
50 and firn compaction must first have ~~could have first~~driven ~~weakened~~ these ice shelves  
51 ~~intotowards~~ a state liable to collapse by weakening the ice and enabling meltwater to pool on  
52 the ice surface. Apparently following the southward progression of ice-shelf instability on the  
53 AP, satellite altimetry shows that the surface of Larsen C Ice Shelf (LCIS) has lowered in recent  
54 decades (Shepherd et al., 2003; Pritchard et al., 2012; Paolo et al., in press). The lowering is  
55 known to be more rapid in the north of LCIS (Figure 1; updated from Fricker and Padman,  
56 2012, as described in section 2) ~~(Paolo et al., in press)~~. Ice flow in this northern region has also

57 accelerated slightly, which may be related to a decrease in back-stress from Bawden Ice Rise  
58 following an iceberg calving in 2004/5 (Haug et al., 2010; Khazendar et al., 2011). However,  
59 the origin of the lowering remains uncertain. Since the ice shelf is floating, the lowering could  
60 be caused by a loss of firn air of nearly the same magnitude, a loss of solid ice approximately  
61 10 times larger, or a combination of the two. ~~(Jansen et al., 2015)~~ With recent evidence of  
62 unusual rifting apparently threatening the stability of LCIS (Jansen et al., 2015), ~~there~~ there is an  
63 urgent need to understand the cause of this long-term lowering in order to project the possible  
64 future ~~collapse~~ of LCIS and the impacts of its many glacier catchments upon sea-level rise and  
65 ocean freshening.

66  
67 The LCIS lowering was initially attributed to increased oceanic basal melting (i.e. ice loss) on  
68 the basis that firn compaction from derived surface melting trends was insufficient to account  
69 for the signal (Shepherd et al., 2003). However, sparse observations of the ocean beneath LCIS  
70 found the ocean to be at or below the sea-surface freezing temperature, suggesting that it is ~~not~~  
71 ~~capable of rapid melting~~ only capable of slow melting (Nicholls et al., 2012). Observations of  
72 the meltwater emanating from the cavity (Nicholls et al., 2004) and widespread marine ice in  
73 LCIS (Holland et al., 2009; Jansen et al., 2013; McGrath et al., 2014) suggest that these  
74 temperatures are spatially and ~~temporally-historically~~ prevalent. Ocean waters entering the  
75 LCIS cavity appear to be constrained to the surface freezing temperature by nearby sea-ice  
76 formation. Since the Weddell Sea has consistently high rates of sea-ice production it has been  
77 regarded as hard to conceive of an ocean warming sufficient to increase melting enough to  
78 explain the lowering (Nicholls et al., 2004). However, year-round sonar measurements ~~at a~~  
79 ~~single location~~ near Kenyon Peninsula in the south of LCIS yield a mean melt rate of ~0.8 m/y  
80 (with a range of 0—1.5 m/y), which is significantly higher and more variable than expected  
81 (K.W. Nicholls, personal communication 2014; Nicholls et al., 2012). Furthermore, ocean data

82 collected in January 1993 from the LCIS ice front (Bathmann et al., 1994) show anomalous  
83 waters that are considerably warmer than any subsequently observed in the cavity or inferred  
84 as sources for melting (Nicholls et al., 2004; Nicholls et al., 2012). If they entered the cavity,  
85 such warm waters could produce a melting anomaly large enough to significantly perturb the  
86 LCIS ice mass budget. Given our incomplete understanding of ocean processes and melting  
87 beneath LCIS, oceanic thinning of LCIS remains a credible explanation for the lowering.

88

89 On the other hand, there is some evidence supporting a hypothesis that the lowering results  
90 from an atmosphere-driven increase in firn compaction (i.e. air loss), either through dry  
91 compaction or through firn melting and refreezing. In general, the AP has experienced strong  
92 atmospheric warming since the 1950s (Marshall et al., 2006; Turner et al., 2014). A spatial  
93 correspondence between ice-shelf collapses and mean atmospheric temperature suggests that  
94 atmospheric warming may have pushed some ice shelves beyond a thermal limit of viability  
95 (Morris and Vaughan, 2003); and the northern edge of LCIS is at this limit. Observations of  
96 LCIS firn-air thickness confirm that there is sufficient firn air available for compaction, that  
97 lower firn-air spatially corresponds with higher melting, and that the northward-intensified  
98 surface lowering spatially corresponds to areas of high melting and firn compaction (Holland  
99 et al., 2011; Trusel et al., 2013; Luckman et al., 2014). Modelled firn compaction entirely offset  
100 the lowering in one study of 2003—2008 (Pritchard et al., 2012), albeit with a high uncertainty.

101 A temporal correspondence between high annual melting and ice shelf collapse (van den  
102 Broeke, 2005) would be expected to hold also for firn compaction before collapse. However,  
103 attributing the lowering to simple atmospheric temperature trends is not straightforward.  
104 Observed AP surface melt days and modelled meltwater fluxes both lack significant trends  
105 during 1979—2010 and have trends that are strongly negative during 1989—2010 (Kuipers  
106 Munneke et al., 2012a). An Automatic Weather Station on LCIS lacks any significant 1985—

107 2011 trend in air temperature in any season (Valisuo et al., 2014), and there is no convincing  
108 evidence of trends in melting derived from reanalysis models during recent decades (Valisuo  
109 et al., 2014). Even without a trend in atmospheric forcing within recent decades, the period  
110 could still be anomalous relative to the long-term mean, and so an atmosphere-driven lowering  
111 remains viable.

112

113 In summary there is a wealth of circumstantial evidence related to the lowering, but no direct  
114 test of its origin. In this study we analyse repeated radio-echo sounding surveys of LCIS,  
115 applying a novel method to separate changes in ice thickness from changes in firn-air thickness  
116 (Holland et al., 2011). The method is presented in section 2 and its results in section 3. We then  
117 consider whether the uncertainties in these ice and air trends are sufficiently well-constrained  
118 to isolate the origin of the LCIS lowering (section 4), and speculate upon the prognosis for the  
119 ice shelf's future stability (section 5).

120

## 121 **2. Method**

122 Radar sounding provides the two-way travel time (TWTT) of a radar wave between the ice-  
123 shelf surface and base. This can be combined with accurate measurements of surface elevation  
124 to derive separate thicknesses of the solid ice and englacial firn air that comprise an ice shelf  
125 (Holland et al., 2011). With multiple surveys it is therefore possible to determine differences  
126 in ice and air thickness over time. There have been many radar surveys of LCIS, but we find  
127 that a very large number of observations are needed to sufficiently reduce the random error in  
128 the ice and air differences. Therefore, only repeated survey lines provide usable data; inter-  
129 survey cross-overs are not sufficient. Fortunately, a nearly meridional (across-ice flow) survey  
130 line sampling the centre of LCIS has been occupied eight times between 1998 and 2012 by  
131 airborne and ground-based radar surveys (Figure 1b, Table 1), offering the opportunity to

132 derive interannual trends in ice and air thickness from these data. The survey line also passes  
133 through five satellite cross-overs of European Space Agency radar altimeter missions, allowing  
134 direct comparison to the known lowering.

135

## 136 **2.1 Theory**

137 We separate the total ice-shelf thickness into its constituent thicknesses of solid ice and firm air  
138 by following the method of Holland et al. (2011), with a few modifications. Since the floatation  
139 of an ice shelf and the propagation of a radar wave through an ice shelf both depend upon the  
140 relative proportions of ice and air, we formulate two corresponding equations from which two  
141 unknown quantities, ice and air thickness, are derived. The presence of a third unknown, liquid  
142 meltwater, is neglected on the basis that most surveys were undertaken early in the austral  
143 spring and there is no evidence of a perennial aquifer in LCIS (see section 4.3).

144

145 If the ice is freely floating then the hydrostatic ice and ocean forces must balance at the ice  
146 base, so the total mass of the shelf ice and firm air equals that of the atmosphere and ocean  
147 displaced

148

$$149 \quad \rho_i I + \rho_a A = \rho_A S + \rho_o (I + A - S). \quad (1)$$

150

151 Here  $I$  is the total solid ice thickness,  $A$  is the total firm air thickness,  $S$  is the ice freeboard  
152 (surface elevation above sea level), and  $\rho_i = 918 \text{ kg m}^{-3}$ ,  $\rho_a = 2 \text{ kg m}^{-3}$ ,  $\rho_A = 1.3 \text{ kg m}^{-3}$ , and  $\rho_o$   
153  $= 1028 \text{ kg m}^{-3}$ , are densities of solid ice, englacial air (partly pressurised), atmospheric air, and  
154 ocean respectively, which are all assumed constant. Adopting a similar approach and separating  
155 the radar delay of ice from that of air using the simple, empirical Complex Refractive Index  
156 Method (e.g. Arcone, 2002), the TWTT of a radar wave through the ice shelf is

157

158

$$T = \frac{2}{c}(n_i I + n_a A), \quad (2)$$

159

160 where  $T$  is the TWTT,  $c = 3 \times 10^8 \text{ m s}^{-1}$  is the speed of light *in vacuo* and  $n_i = 1.78$  and  $n_a = 1.0$

161 are refractive indices of pure ice and air. Combining (1) and (2) and eliminating variables as

162 appropriate, we obtain expressions for the constituent ice and air thicknesses (and hence total

163 thickness,  $I+A$ ) as functions of known quantities and the measured TWTT and surface

164 elevation:

165

$$A = \left[ \frac{c(\rho_o - \rho_i)}{2n_i} T + (\rho_A - \rho_o) S \right] / \left[ (\rho_a - \rho_o) + \frac{n_a(\rho_o - \rho_i)}{n_i} \right] \quad (3)$$

$$I = \left[ \frac{c(\rho_o - \rho_a)}{2n_a} T + (\rho_A - \rho_o) S \right] / \left[ (\rho_i - \rho_o) + \frac{n_i(\rho_o - \rho_a)}{n_a} \right]. \quad (4)$$

168

169 Taking the temporal derivative of these expressions, we obtain the trends in ice and air

170 thickness as a function of the trends in elevation and TWTT:

171

$$\frac{\partial A}{\partial t} = \left[ \frac{c(\rho_o - \rho_i)}{2n_i} \frac{\partial T}{\partial t} + (\rho_A - \rho_o) \frac{\partial S}{\partial t} \right] / \left[ (\rho_a - \rho_o) + \frac{n_a(\rho_o - \rho_i)}{n_i} \right] \quad (5)$$

$$\frac{\partial I}{\partial t} = \left[ \frac{c(\rho_o - \rho_a)}{2n_a} \frac{\partial T}{\partial t} + (\rho_A - \rho_o) \frac{\partial S}{\partial t} \right] / \left[ (\rho_i - \rho_o) + \frac{n_i(\rho_o - \rho_a)}{n_a} \right]. \quad (6)$$

174

175 Hence, we calculate ice and air trends directly from elevation and TWTT trends; we do not

176 derive the ice and air thickness for each survey and then calculate their trends. This explicitly

177 excludes potentially large errors inherent in steady corrections to the input data, particularly

178 from the geoid and mean dynamic ocean topography. Evaluating the known quantities in these

179 terms(5)—(6), we find that

180

181 
$$\frac{\partial A}{\partial t} = 1.06 \frac{\partial S}{\partial t} - 0.114 \frac{c}{2n_i} \frac{\partial T}{\partial t} \quad (7)$$

182 
$$\frac{\partial I}{\partial t} = -0.598 \frac{\partial S}{\partial t} + 1.06 \frac{c}{2n_i} \frac{\partial T}{\partial t}, \quad (8)$$

183

184 where the TWTT is expressed as a solid ice equivalent for clarity.

185

186 Note that the derivation of (5)—(6) from (3)—(4) neglects temporal derivatives of all densities,  
 187 of which the most variable is the ocean density. Repeating the derivation and retaining ocean  
 188 density terms provides an expression in which 0.3 m/y ice loss would require a  $\sim 2 \text{ kg m}^{-3} \text{ year}^{-1}$   
 189 <sup>1</sup> reduction in ocean density, and 0.03 m/y air loss would require a  $\sim 0.1 \text{ kg m}^{-3} \text{ year}^{-1}$  increase  
 190 in ocean density. Such changes persisting over 15 years are clearly implausible, and we  
 191 conclude that ocean density changes have negligible effect.

192

## 193 **2.2 Application to Larsen C Ice Shelf**

194 We apply the [above](#) method to eight radar surveys between February 1998 and December 2012  
 195 along a line traversing the centre of LCIS (Figure 1b, red line). The surveys were carried out  
 196 by ground-based field parties and a variety of aircraft flying at different heights and speeds,  
 197 and many different radar instruments and methods for measuring elevation were used (Table  
 198 1). The processed elevation and TWTT data are shown in Figures 2a and 2b. The most densely-  
 199 spaced TWTT data were gathered during the 2004 NASA-CECS airborne survey, so this is  
 200 chosen as a baseline dataset. For each elevation and TWTT measurement in the other surveys,  
 201 we find the difference from the nearest corresponding measurement in the 2004 survey,  
 202 discarding all observations that do not have a 2004 analogue within 1000 m. These elevation  
 203 and TWTT differences are shown in Figures 2c and 2d. There is a great deal of scatter in the  
 204 differences, which could result from several factors, including the advection of ice topography  
 205 across the survey line at  $\sim 400 \text{ m/y}$  (Rignot et al., 2011). The differences are therefore binned

206 spatially to extract the overall signals by averaging random noise, and linear trends in surface  
207 elevation and TWTT are calculated for the bins. Equations (5) and (6) are then used to  
208 determine the trends in ice and firn-air thickness from trends in surface elevation and TWTT.  
209 We apply this methodology in two ways, first considering the overall trends for the entire  
210 survey line, and then dividing the survey into five bins, surrounding each of the five satellite  
211 crossover points (Figure 1).

212

213 The 2012 British Antarctic Survey (BAS) ground-based survey was a mission of opportunity  
214 within a wider seismic season (Brisbourne et al., 2014) and deviated from the rest of the  
215 surveys, heading due south (Figure 1b, yellow line). However, it did repeat a flight line from  
216 the 1998 BAS airborne survey, so to include the data we first calculate the mean difference  
217 between the 2012 and 1998 surveys along the meridional line, and then the mean difference  
218 between the 2004 and 1998 surveys along the primary line, and then use these to obtain the  
219 2012—2004 difference. The results are only included in the northernmost bin when we  
220 consider along-survey variability; they are not included in the whole-survey results.

221

### 222 **2.3 Radio-echo sounding survey data**

223 Different techniques are available for picking radar return echoes from echograms, and so to  
224 ensure that our inter-survey trends are as robust as possible the ice surface and base echoes  
225 from all surveys were re-picked in a consistent manner. Automatic first-break picks on time-  
226 windowed and scaled traces were manually edited to remove or correct mis-picks. For airborne  
227 surveys, TWTT was calculated as the difference between ice surface and basal returns from the  
228 ice-penetrating radar, thus minimising inter-survey biases by removing any error associated  
229 with the absolute accuracy of the radar. Basal return TWTTs from the ground-based survey  
230 data were corrected for the radar antenna separation. In the NASA IceBridge 2009 and 2010

231 and BAS 2011 airborne surveys, the altitude of the aircraft in specific sections caused the  
232 surface multiple return to appear at a TWTT similar to that of the basal return, significantly  
233 contaminating the picks. Therefore, the radargrams were overlain with an estimate of the  
234 surface multiple return calculated from the aircraft altitude and also an estimate of the basal  
235 return derived from the aircraft altitude, surface elevation and hydrostatic assumption.  
236 Wherever the TWTT of these two signals was indistinguishable in the radargram, no basal  
237 return pick was recorded. Significant marine ice bands were omitted from all surveys, because  
238 basal returns become indistinct and the meteoric—marine transition may be visible instead.

239  
240  
241 The TWTT data are recorded with a wide variety of instruments and subject to different  
242 processing techniques to optimise the signal prior to picking. The TWTT precision in the  
243 echogram picked (i.e. the time between samples of return power; the reciprocal of the sampling  
244 rate) varies between surveys, with a mean of ~4 m ice equivalent and a range of 0.13—8.8 m  
245 ice equivalent. The 15-year TWTT change is of comparable magnitude to this precision (see  
246 below). However, the first break of the return echo is actually known at higher precision  
247 because waveform fitting is used to interpolate between samples of the return echo power.  
248 Furthermore, each inter-survey TWTT difference, from which ice and air trends are calculated,  
249 is actually the mean of a population of thousands of individual point differences. These  
250 populations are well-resolved by the TWTT precision, and so by using large numbers of data  
251 points we are able to detect mean inter-survey differences statistically at a precision much finer  
252 than that of the individual data.

253  
254 TWTTs from the 2009 IceBridge survey were found to contain consistently shorter radar-wave  
255 delays than the 2009 McGrath ground-based survey despite being collected only two weeks

256 earlier, with a mean ~~ice~~-equivalent ice thickness approximately 10 m ~~lower~~thinner and therefore  
257 a significant outlier relative to the other surveys. The data were investigated and re-picked, but  
258 the problem seems to result from transmit/receive switches not meeting their switching-time  
259 specification in the survey (<https://data.cresis.ku.edu/#RDS>). ~~Therefore, so~~ the 2009 IceBridge  
260 TWTT data are neglected throughout this study, other than in a test recalculation to demonstrate  
261 their effect. The laser altimeter elevation data from this survey are used in all calculations.  
262

## 263 **2.4 Surface elevation survey data**

264 Surveyed ice elevation data have several corrections applied to make them directly comparable.  
265 Corrections for the steady geoid and mean dynamic ocean topography are not required because  
266 the method employs only temporal differences in elevation, as shown by (5) and (6). All data  
267 are de-tided using the CATS2008a\_opt model (L. Padman personal communication 2014) and  
268 have a local sea-level rise of 4 mm/y removed (Rye et al., 2014).

269  
270 Most of the instruments used to derive elevation were well-calibrated in the field (e.g.  
271 <http://nsidc.org/data/docs/daac/icebridge/ilatm2/index.html>), but the two BAS airborne  
272 surveys in 1998 and 2011 were not calibrated to the centimetre-scale accuracy required here.  
273 The 1998 survey passed over the open ocean in many locations, so these elevations were  
274 corrected for tides, EIGEN-6C geoid (<http://icgem.gfz-potsdam.de/ICGEM/ICGEM.html>), and  
275 DTU12 mean dynamic topography  
276 ([http://www.space.dtu.dk/english/Research/Scientific\\_data\\_and\\_models/downloaddata](http://www.space.dtu.dk/english/Research/Scientific_data_and_models/downloaddata)), and  
277 then the mean difference from zero (sea surface) of 1.01 m was removed from the entire dataset.  
278 Repeating this procedure for the 2011 survey produced a 1.33 m offset, but from only a small  
279 area of open-ocean data. Fortunately, it was possible to correct the 2011 elevations to match  
280 the well-calibrated 2010 NASA IceBridge laser altimeter survey that took place 10 weeks

281 earlier. However, this was complicated by the issue of radar firm penetration, a progressive  
282 southward decrease in the difference between surveys (Figure 3). Radar altimetry penetrates  
283 the surface and reflects from within the firm layer, whereas laser altimetry reflects from the  
284 surface. North of 67.85 °S there is no broad-scale spatial variation in the offset between datasets  
285 (Figure 3), implying either uniform or no radar penetration. We regard subtract the mean offset  
286 in this area, 1.59 m, as the calibration error and subtract it from the 2011 data everywhere and  
287 then treat the variable radar penetration to the south separately.

288  
289 The elevation estimates derived from the two BAS radar altimeter surveys need a firm-  
290 penetration correction to make them comparable to those derived from the laser altimeters and  
291 GPS. After the above calibration, the 2011 radar altimeter survey records a progressively lower  
292 surface than the 2010 laser altimeter survey to the south of 67.85 °S, so which we ascribe we  
293 ascribe this southward decrease to firm penetration by the radar altimeter in the 2011 survey, .  
294 This is qualitatively consistent with the known southward increase in firm air content (Holland  
295 et al., 2011). ~~North of 67.85 °S there is no broad-scale spatial variation in the offset between~~  
296 ~~datasets, implying either uniform or no radar penetration. We subtract the mean offset in this~~  
297 ~~area, 1.59 m, from the 2011 data and then treat the variable radar penetration to the south~~  
298 ~~separately.~~

299  
300 ~~The elevation estimates derived from the two BAS radar altimeter surveys need a firm-~~  
301 ~~penetration correction to make them comparable to those derived from the laser altimeter and~~  
302 ~~GPS. This correction consists~~ Therefore, we correct both the 1998 and 2011 radar altimeter  
303 surveys by adding of a linear fit south of 67.85 °S to the difference between the IceBridge 2010  
304 and BAS 2011 surveys (Figure 3). Thus, out Out of necessity, the correction includes implicit

305 assumptions that there is no firm penetration north of this during either radar survey, and that  
306 penetration to the south ~~did not change~~ is identical in-between February 1998 and January 2011.

307

## 308 **2.5 Satellite radar altimeter elevation data**

309 Satellite radar altimeter data are used to corroborate the surveyed elevation data and provide a  
310 context for the lowering. The satellite elevation timeseries combine radar altimeter data from  
311 the ERS-1, ERS-2, and Envisat satellites using an existing methodology (Fricker and Padman,  
312 2012) but including new data to the end of 2011. These data consist of repeat measurements of  
313 ice-shelf surface elevation at satellite orbit crossing points, available approximately every 35  
314 days during Austral winters (April—November) during 1992—2011.

315

316 When analysing the data we found a strong correlation between changes in elevation and  
317 changes in surface backscatter for the period 1992—1993 (the first two years of ERS-1). This  
318 anomalous behaviour in the altimeter backscatter, which alters the shape of the waveform from  
319 which the elevation is deduced, occurs throughout Antarctica. This leads us to believe that  
320 these data may not be reliable, so we only use data from 1994 onwards in this study. Shepherd  
321 et al. (2010) and Paolo et al. (in press) also neglected data prior to 1994 in their  
322 ~~analysis~~ analyses. This is important because ~~other~~ studies of LCIS that include these early data  
323 ~~(Shepherd et al., 2003; Fricker and Padman, 2012) derive~~ have very rapid lowering in the 1990s  
324 ~~(Shepherd et al., 2003; Fricker and Padman, 2012)~~ that is not found if the early data are  
325 neglected ~~supported by the remaining data~~. To illustrate the lowering of LCIS we first consider  
326 the period 1994—2011 (Figure 1a), though our main analysis focuses upon the 1998—2011  
327 period covered by the radar surveys (Figure 1b). During the latter period the LCIS lowering  
328 has the same general pattern, but the trends at the five crossovers covered by the survey line

329 are slightly different. Importantly, the survey line does not sample the northern section of LCIS  
 330 in which the fastest lowering occurs.

331

332 To compare elevation trends derived from the survey data to those derived from satellite radar  
 333 altimeter data (Figure 4 and Table 2) a single satellite elevation trend was derived that  
 334 represents all five independent satellite crossovers. First, the mean elevation for the Austral  
 335 winter of 1998 was calculated for each independent crossover and subtracted from each  
 336 crossover's time series. The resulting temporal elevation anomaly data were then treated as  
 337 individual data points in a single merged time series, and from that a linear trend was calculated  
 338 to compare to the surveyed trends. Linear trends were also calculated at each crossover, as  
 339 presented in Figures 1, 5, 6, and 7.

340

## 341 2.6 Ice and air mass balances

342 We consider the derived ice and air losses in the context of the ice and air mass balances of  
 343 LCIS. The mass balance of the ice fraction of the ice shelf (i.e. excluding firn air) yields an  
 344 equation governing the depth-integrated ice thickness

345

$$346 \left| \frac{\partial I}{\partial t} + I \nabla \cdot \mathbf{u} + \mathbf{u} \cdot \nabla I = a_I - m_{Ib} \right. \quad (9)$$

347

348 where  $\mathbf{u}$  is the two-dimensional horizontal ice velocity vector,  $a_I$  is net surface ice  
 349 accumulation, and  $m_{Ib}$  is basal melting. The mass balance of the air fraction of the ice shelf  
 350 yields a similar equation for depth-integrated air thickness

351

$$352 \left| \frac{\partial A}{\partial t} + A \nabla \cdot \mathbf{u} + \mathbf{u} \cdot \nabla A = a_A - m_{As} - d \right. \quad (10)$$

353

354 where  $a_A$  is the air trapped in the firn by accumulation,  $m_{sA}$  is the loss of air by surface melting,  
355 percolation, and refreezing, and  $d$  is the loss of air by dry compaction. The terms on the left-  
356 hand side of both equations are the unsteady term, divergence, and advection.

357

358 When analysing the results we map the terms in the ice mass balance (9) following a previous  
359 study (McGrath et al., 2014) that combined data from several sources. Divergence, advection,  
360 and mass input terms can be mapped from satellite-based observations of ice velocity (Rignot  
361 et al., 2011) and ice-shelf elevation (Griggs and Bamber, 2009), firn-air thickness derived from  
362 airborne radar measurements (Holland et al., 2011), and model estimates of net surface  
363 accumulation (Lenaerts et al., 2012). Though we also possess a spatial map of ice surface  
364 elevation change, an unknown fraction of this is caused by firn-air changes and so we cannot  
365 derive ice thickness change outside the temporal and spatial range of our survey data.  
366 Neglecting the unsteady term, we can derive a map of steady-state melting from the other terms.  
367 Prior to these calculations the ice thickness and velocity fields are smoothed over a 20-km  
368 footprint (masked outside the ice shelf) to remove small-scale noise that is amplified in the  
369 spatial derivatives. The firn-air mass balance (10) contains so many unknown quantities that  
370 we do not attempt to derive its terms.

371

### 372 **3. Results**

373 We first present the main results of the study, before a full analysis of the uncertainties in  
374 section 4.

375

#### 376 **3.1 Trends over the whole survey line**

377 Figure 4 shows the elevation and TWTT for each survey, as mean differences from 2004 over  
378 the entire survey line, and Table 2 gives the ‘primary’ derived trends for these ‘reference’ data

379 and also a variety of alternatives. Since the data points and their error bars refer to differences  
380 from 2004, the 2004 data are zero for both elevation and TWTT, with zero error. The surveyed  
381 elevation differences show a lowering trend ( $-0.066 \pm 0.017$  m/y) that is very similar to that  
382 obtained from the satellite altimeter data ( $-0.062$  m/y); the trends are not expected to be  
383 identical due to method uncertainties and spatial and temporal differences in sampling.  
384 Crucially, there is also a decreasing trend in surveyed TWTT ( $-0.296 \pm 0.17$  m/y ice equivalent),  
385 though there is considerably more inter-survey scatter in this quantity and uncertainty in the  
386 resulting trend (see section 4.3). Combining these observed trends using (5) and (6) reveals that  
387 the surface lowering is caused partly by a combination of air loss ( $-0.0367 \pm 0.026$  m/y) and  
388 partly by ice loss ( $-0.274 \pm 0.18$  m/y). The ice loss has a much greater magnitude, but the Ice loss  
389 is an order of magnitude larger than air loss, but surface lowering is approximately ten times  
390 more sensitive to air loss than ice loss, so ice and air loss, so that ice loss and air loss contribute  
391 approximately equally to the surface lowering. There is considerable scatter in the data and  
392 several sources of uncertainty in the methodology, but our conclusion that ice and air loss both  
393 contribute to the lowering is robust when several different combinations of data are used in the  
394 calculations (see section 4).

395

### 396 **3.2 Variation within survey line**

397 We now consider spatial variability by binning the survey data around each satellite crossover  
398 (Figure 5a). The derived ice loss is reasonably uniform along the line, while the derived air loss  
399 is noticeably higher towards the southern end of the survey line. However, the surveyed  
400 elevation trends at the southern end of the line show considerably more lowering than the  
401 satellite elevation trends. Inspection of the data underlying the timeseries in each bin (Figure  
402 6) reveals that the surveyed elevations are reasonable apart from the 1998 data in the  
403 southernmost bin (centred on  $68.3^\circ\text{S}$ ), which exceed the range of the figure. We consider the

404 satellite altimeter data to be a more reliable measure of lowering because the 1998 surveyed  
405 elevation data are subject to calibration and firn-penetration corrections that are uncertain in  
406 this area (see section 2.4). The TWTT data are not subject to these uncertain corrections, so we  
407 retain these and recalculate the ice and air trends with Replacing the surveyed elevation trends  
408 replaced by with the satellite elevation trends (Figure 7a). This has virtually no effect on the  
409 derived ice loss, but removes the air loss completely from the southernmost bin, so that the air  
410 loss is concentrated on the centre of the survey line.

411

412 The air and ice losses shown in Figures 5a and 7a are scaled so that their resultant surface  
413 lowering can be read on the left-hand axis. ~~From~~ Figure 7a ~~suggests we conclude~~ that air loss  
414 contributes the majority of the lowering in the centre of the survey line, while ice loss also  
415 contributes to this lowering and is responsible for the lowering at both ends. It is unsurprising  
416 that the ice and air loss have different spatial patterns, given their different (oceanic, ice-  
417 dynamic, and atmospheric) forcings.

418

### 419 **3.3 Ice and air budgets**

420 Figure 8 shows the maps of each term in the LCIS ice mass balance (9). Thinning along  
421 flowlines causes a sink of ice through divergence (Figure 8a), advection is generally a source  
422 of ice where the ice shelf flows from thick to thin (Figure 8b), and modelled surface  
423 accumulation is almost uniform (Figure 8c). Their sum, the steady melting map (Figure 8d),  
424 contains obvious artefacts but also many features that match our existing knowledge of ocean  
425 melting beneath LCIS. For example, the results are in agreement with a simple ocean-layer  
426 model (Holland et al., 2009) that predicts strong melting along the grounding line and freezing  
427 in the thinner ice immediately offshore of islands and peninsulas on the western coast (also  
428 visible as negative values in the advection term). A more sophisticated three-dimensional ocean

429 model (Mueller et al., 2012), forced only by tides, predicts large values of tidally-driven  
430 melting next to Bawden Ice Rise and Kenyon Peninsula, which also seem apparent in Figure  
431 8d, though other areas of high melting near the ice front and south of Kenyon Peninsula are not  
432 consistent with the model.

433

434 Combining the estimated mean terms in the ice mass budget (Figure 8) with the ice loss derived  
435 along the survey line (Figures 5a and 7a) allows us to consider the full unsteady ice budget  
436 (Figure 5b and 7b). The basic ice balance is between accumulation and divergence, with  
437 advection becoming important at the southern end of the line. If the ice shelf were in steady  
438 state the derived oceanic melt rate would be an order of magnitude smaller than accumulation  
439 and divergence (0.06 m/y). In fact, our derived ice loss profiles suggest a mean oceanic melt  
440 rate over the survey line of 0.26 m/y, peaking at 0.5 m/y in the southernmost bin. These  
441 estimates are consistent with modelled patterns of melting (Holland et al., 2009; Mueller et al.,  
442 2012) and observations in a higher-melting region nearby (K.W. Nicholls, personal  
443 communication 2014; Nicholls et al., 2012). Crucially, without basal melting the components  
444 of the mass budget are approximately balanced, so the majority of the melting is causing net  
445 ice loss. This emphasizes that for ice shelves melted by cold ocean waters, relatively small  
446 absolute changes in melting can have a significant influence on the ice shelf mass balance. In  
447 comparison, warm-water ice shelves such as Pine Island Glacier can have much larger melting  
448 perturbations (e.g. 5 m/y; Wingham et al., 2009), causing ~~equally~~correspondingly large  
449 thinning rates, but these perturbations are a much smaller fraction of the mean melt rate (e.g.  
450 100 m/y; Dutrieux et al., 2013).

451

452 The terms in the analogous firn-air budget are extremely uncertain. To put the derived air loss  
453 of 0.04 m/y into context, we simply note that there was 10—15 m of air in the surveyed section

454 during the 1997/98 survey (Holland et al., 2011), and if fresh snow is deposited at a density of  
455 350—450 kg m<sup>-3</sup> (Kuipers Munneke et al., 2012b) then the accumulation of 0.5 m/y ice implies  
456 the addition of 0.5—1 m/y firn air each year before compaction is taken into account.  
457 Therefore, our best estimate is that the net air loss is only 5-10% of the annual air input.

458

#### 459 **4. Error estimation**

460 The data contain a considerable amount of scatter and their interpretation relies upon a clear  
461 understanding of the uncertainties inherent in the derived trends. For this reason, we present a  
462 thorough error analysis before proceeding to discuss the implications of our findings. This  
463 analysis starts with a simple technique for visually assessing the reliability of the results, before  
464 proceeding to more formal methods.

465

#### 466 **4.1 Visual Assessment**

467 It is possible to visually assess the reliability of ice and air trends from appropriately-plotted  
468 trends in elevation and TWTT. If the TWTT trend is expressed as a solid-ice surface-elevation  
469 equivalent, i.e.

470

$$471 \quad \frac{\partial T_s}{\partial t} = \frac{c}{2n_i} \frac{\rho_o - \rho_i}{\rho_o - \rho_A} \frac{\partial T}{\partial t}, \quad (11)$$

472

473 then comparing  $\partial T_s / \partial t$  to the elevation trend  $\partial S / \partial t$  allows us to determine the value of  $\partial A / \partial t$   
474 from (5). Any elevation trend that is more negative than  $\partial T_s / \partial t$  implies a loss of air, with the  
475 air loss equal to 1.06 times the difference between  $\partial S / \partial t$  and  $\partial T_s / \partial t$ . For this purpose, the  
476 two y-axes of Figures 4, 5a, 6, and 7a are scaled such that the left-hand axis shows both ice  
477 surface elevation ( $\partial S / \partial t$ ) and TWTT expressed as solid-ice surface equivalent ( $\partial T_s / \partial t$ ).

478 Consideration of the numerator of (6) shows that  $\partial T_s / \partial t$  merely has to be more negative than

479  $-0.107 \times \partial S / \partial t$  to imply a loss of ice; any  $\partial T_s / \partial t$  that is negative enough to be distinguished  
480 in the figures implies some ice loss. In plain terms, Figure 4 is scaled such that if the red line  
481 (scaled TWTT trend) is parallel to the green line (elevation trend) then the lowering is due  
482 solely to ice loss, and if the red line is flat then all of the lowering is due to air loss.

483

484 These criteria allow a simple visual assessment of the signal present in the available data. Our  
485 assessment of Figure 4 is that the scaled TWTT is decreasing, but that this result is not robust  
486 in the sense that it is dependent upon all datasets and removing certain surveys would remove  
487 the ~~decrease~~calculated trend. This reduces confidence in the conclusion that ice loss has  
488 occurred. On the other hand, we do not believe that the scaled TWTT data could support a trend  
489 that is more negative than the elevation trend, and therefore we are confident in our conclusion  
490 that air loss has occurred.

491

492 A formal analysis revisits these conclusions below, but this requires many assumptions about  
493 the nature of the errors and so is not necessarily superior. There are many sources of error in  
494 our surveys, which we divide into two classes. The first class of errors produces random intra-  
495 survey scatter, which affects the extent to which the data from each survey estimate the mean  
496 signal within that survey. The second class of errors create a systematic signal across a whole  
497 survey, directly affecting inter-survey differences. The latter are of greatest concern because  
498 they have the largest effect on trends.

499

## 500 **4.2 Intra-survey errors**

501 Predominantly intra-survey errors include:

- 502 • Instrument and processing error (including radar picking error, assumed intra-survey  
503 because all surveys were re-picked consistently).

- 504 • Spatial offset from the 2004 survey reference line (there is no systematic spatial  
505 difference between surveys, but the data deviate from a straight line within surveys, and  
506 the mean east—west gradients in ice thickness and firn air thus induce intra-survey  
507 error).
- 508 • Advection of complex ice topography through the survey line (assumed intra-survey  
509 because ice features are smaller than both the along-survey distance and the advection  
510 lengthscale in the across-survey direction: 15 years  $\times$  400 m/y).

511

512 We can easily quantify these random errors by considering, for each survey, the statistics of  
513 each population of differences of data points from their 2004 analogues (Table 3). Standard  
514 deviations are relatively large, 1—2 m for elevation and  $\sim$ 10 m ice equivalent for TWTT, as  
515 expected from previous analyses of the error in individual point measurements (Holland et al.,  
516 2009). However, when all data are considered the standard errors are small due to the large  
517 sample sizes. Assuming that the differences are independent and normally distributed, 95%  
518 confidence interval bounds for the survey mean are given by multiplying the standard error by  
519 1.96, as shown by the error bars in Figure 4. We estimate overall 95% confidence interval  
520 bounds as  $\pm 0.04$  m for elevation and  $\pm 0.5$  m ice equivalent for TWTT. Thus, from a random  
521 error perspective, we are confident that all surveys differ significantly from 2004 apart from  
522 the elevation differences in the 2011 and McGrath 2009 surveys and both elevation and TWTT  
523 datasets in 2012. Simple examination of the error bars in Figure 4 shows that variation within  
524 these random error bounds will have negligible effect on the computed trends.

525

### 526 **4.3 Inter-survey errors**

527 Predominantly inter-survey errors include:

- 528 • Differences between survey instruments, calibration, and processing (radar altimeter  
529 penetration, ice-penetrating radar power and frequency, speed and altitude of  
530 acquisition platform).
- 531 • Time-variable presence of liquid meltwater in the firn column.
- 532 • Time-variable firn penetration in the ice-penetrating radar surface pick.
- 533 • The time-variable part of dynamic ocean topography (inter-survey because most  
534 surveys are rapid compared to the relevant variations in ocean flow; affects elevation  
535 only).
- 536 • Error in the tidal model correction (inter-survey because most surveys are rapid  
537 compared to tides; affects elevation only).
- 538 • The inverse barometer effect (inter-survey because most surveys are rapid compared to  
539 the relevant variations in atmospheric pressure; affects elevation only).

540

541 An initial concern is that the NASA IceBridge and NASA-CECS surveys (high-altitude, high-  
542 speed, consistent radar systems, laser altimeter) differ from the BAS airborne surveys (lower-  
543 altitude, slower, different radar, radar altimeter) and both differ from the ground-based surveys  
544 (low-frequency radar, GPS elevation). However, the three types of survey are interleaved in  
545 time, so such differences do not necessarily cause systematic trends. The issue is assessed by  
546 re-calculating the trends using different combinations of data (Table 2). Considering only the  
547 two BAS surveys produces broadly the same results. However, considering only NASA  
548 IceBridge and NASA-CECS surveys produces a much weaker surface lowering and no  
549 decrease in TWTT, so that the ice loss disappears. Systematically removing the surveys from  
550 the calculation reveals that it is neglecting the BAS 1998 survey that removes these trends  
551 (Table 2). We know of no reason to neglect this survey, but this suggests that we treat TWTT  
552 and ice trends with additional caution.

553

554 The presence of meltwater in the firm would require us to adapt the methodology because it  
555 affects both the hydrostatic floatation and radar-wave delay of the ice shelf, as described by  
556 Holland et al. (2011), leading to different ice and air thicknesses being derived from the same  
557 TWTT and elevation. This potentially confounding issue is neglected because most surveys  
558 were sampled in November, before the onset of melt (Barrand et al., 2013), and instrumented  
559 boreholes have revealed no evidence of a perennial aquifer (K. W. Nicholls and B. Hubbard,  
560 personal communications, 2015). However, the two BAS surveys were sampled in summer and  
561 could be contaminated by the presence of meltwater. Repeating the derivation of (3) and (4)  
562 but including the effects of meltwater produces new equations from which 0.57 m more air and  
563 5.6 m less ice would be derived for every 1 m of meltwater present (Holland et al., 2011). A  
564 maximum LCIS meltwater content of 0.4 m (Holland et al., 2011) therefore implies a maximum  
565 underestimate of 0.23 m air and overestimate of 2.24 m ice. The summer of 1997/98 was a high  
566 melting year (Tedesco, 2009), and if meltwater was present during the 1998 survey the derived  
567 air content should be higher and ice content lower, enhancing the air loss trend and reducing  
568 the ice loss trend. A linear regression to 0.23 m air error and -2.24 m ice error in 1998 and no  
569 meltwater-derived error in the other surveys yields maximum trend errors of -0.0137 m/y air  
570 and +0.134 m/y ice. Melt estimates for 2010/11 are not available, but any 2011 meltwater  
571 would have the opposite effect on the inter-survey trends to 1998 meltwater, and thus mitigate  
572 this issue.

573

574 For the airborne surveys, surface penetration could affect both radar altimeters and the surface  
575 pick of ice-penetrating radars. We have used a penetration correction in radar altimeter data  
576 (see above), and their agreement with the satellite elevation trend implies that deviation from  
577 this correction is not important. Our strategy of finding the ice TWTT by picking the surface

578 and basal returns and differencing the result means that surface penetration could affect the  
579 TWTT. We examine this by comparing the radar surface picks with altimeter data. This test is  
580 imperfect because it introduces errors from the aircraft altitude and surface elevation data, and  
581 requires absolute accuracy in the radar data that is not needed of the TWTT differences used.  
582 The test cannot even be performed for the NASA IceBridge and NASA-CECS surveys because  
583 the absolute timing of the radar pulse transmission is not known to the required accuracy. The  
584 mean difference between altimeter-derived surface elevations and radar-derived surface  
585 elevations is 2.14 m for the BAS 1998 survey and 2.38 m for the BAS 2011 survey. The  
586 altimeter-derived elevation is higher than the radar-derived elevation in both cases, so the  
587 difference may be caused by surface penetration. This very limited dataset suggests that radar  
588 firn penetration is of order 2 m, with an interannual variability of order 0.2 m.

589

590 These differences between radar surface picks and altimeter data are also the only independent  
591 information we have to quantify overall inter-survey error in TWTT differences. They are again  
592 imperfect in this role because they include error in aircraft altitude and surface elevation data  
593 that does not appear in the TWTT differences used in (5) and (6). Also, if the error in basal and  
594 surface picks is identical (e.g. from an absolute calibration error) then the error in their  
595 difference is zero. On the other hand, if the surface and basal errors are uncorrelated and of the  
596 same magnitude then the TWTT difference error is the surface pick error multiplied by  $\sqrt{2}$ . We  
597 believe that an inter-survey error of 2 m ice equivalent for TWTT is a reasonable compromise,  
598 and this value is in good agreement with the deviation of the TWTT points from the trend line  
599 in Figure 4.

600

601 The effects of unsteady dynamic ocean topography, error in the tidal correction, and inverse  
602 barometer effect should each contribute an inter-survey error of order 0.1 m to the surface

603 elevation differences (L. Padman, personal communication, 2014; Padman et al., 2003; King  
 604 and Padman, 2005). If these errors are uncorrelated, this would create a total error of about 0.2  
 605 m, and this estimate is consistent with both the deviation of the surveys from the linear trend  
 606 and the difference in elevation between the two 2009 surveys (Figure 4). In any case, the  
 607 surface lowering from the satellite crossovers provides an independent test of the surveyed  
 608 elevation trend, and the two trends are only slightly different (Table 2), as might be expected  
 609 from the difference in spatial and temporal sampling.

610

611 Given these overall inter-survey error estimates (0.2 m elevation and 2 m TWTT ice  
 612 equivalent), we used a Monte Carlo approach to estimate the resultant uncertainty in the  
 613 elevation and TWTT trends. The trends were recalculated 500,000 times with all data points  
 614 subject to a perturbation drawn from a normal distribution with 95% confidence interval  
 615 bounds equal to the error estimates. This yields a population of trends with 95% confidence  
 616 interval bounds of  $\pm 0.017$  m/y for elevation trends and  $\pm 0.17$  m/y ice equivalent for TWTT  
 617 trends. Evaluating the terms as in (7) and (8) and combining the errors in quadrature yields

618

$$619 \quad \varepsilon_{At} = \sqrt{0.013\varepsilon_{Tt}^2 + 1.13\varepsilon_{St}^2} \quad (12)$$

$$620 \quad \varepsilon_{It} = \sqrt{1.13\varepsilon_{Tt}^2 + 0.36\varepsilon_{St}^2}. \quad (13)$$

621

622 Where  $\varepsilon_{At}$ ,  $\varepsilon_{It}$  and  $\varepsilon_{St}$  are errors in  $\partial A/\partial t$ ,  $\partial I/\partial t$ , and  $\partial S/\partial t$  respectively. The symbol  $\varepsilon_{Tt}$  represents  
 623 the error in  $c/2n_i \partial T/\partial t$ , TWTT converted to solid ice thickness. These formulae yield  
 624 uncertainties of  $\pm 0.026$  m/y for  $\partial A/\partial t$  and  $\pm 0.18$  m/y for  $\partial I/\partial t$ .

625

#### 626 **4.4 Error summary**

627 In summary, formal error estimates suggest that both the ice and air loss derived in our  
628 reference calculation are robust. However, visual assessment of Figure 4 suggests that the data  
629 support air loss more strongly than ice loss. Recalculating the trends with different  
630 combinations of the data (Table 2) shows that almost all possible calculations have significant  
631 air loss; the only way to obtain insignificant air loss is to include 2009 IceBridge TWTT data  
632 known to be erroneous. On the other hand, removing either the BAS 1998 or McGrath 2009  
633 surveys is sufficient to render the ice loss insignificant. Any meltwater that were present during  
634 the BAS 1998 survey would further strengthen the air loss and weaken the ice loss. Our best  
635 estimate is that the lowering is a result of both air loss and ice loss, but there remains a  
636 possibility that air loss is solely responsible.

637

638 The preceding calculations apply to the whole-survey comparisons shown in Figure 4. The  
639 latitude bins shown in Figures 5—7 contain fewer data, so the intra-survey standard error  
640 should increase. Standard errors scale with the reciprocal square root of the number of  
641 datapoints, so the 95% confidence interval bounds approximately double ( $\pm 0.08$  m for  
642 elevation and  $\pm 1$  m ice equivalent for TWTT) when the data sample size are reduced by a factor  
643 of 5. Inter-survey systematic error should in principle remain similar, but on the shorter length  
644 scale of an individual bin, several intra-survey errors become inter-survey in character  
645 (differences in radar picking, survey path, and advection of ice features, which can be a  
646 significant fraction of a bin length in the along-survey direction). Scrutinising the time series  
647 in Figure 6 suggests a reasonable confidence in the binned trends. In most cases a downward  
648 trend of the TWTT is apparent, suggesting some ice loss has occurred, and the scaled TWTT  
649 data would not support a downwards trend steeper than the satellite elevation, suggesting air  
650 loss has occurred. The steepest elevation trends and shallowest TWTT trends are in the centre  
651 of the survey line, implying greatest air loss.

652

## 653 **5. Discussion**

654 The uncertainties are considerable, but our primary estimate is that the lowering ( $0.066\pm 0.017$   
655 m/y, or  $0.99\pm 0.26$  m) is caused by both ice loss ( $0.28\pm 0.18$  m/y, or  $4.2\pm 2.7$  m) and firn air loss  
656 ( $0.037\pm 0.026$  m/y, or  $0.56\pm 0.39$  m). It is notable that though their effect on the lowering is  
657 approximately equal, ice loss is an order of magnitude larger than air loss. The derivation of  
658 these values allows us to speculate upon the possible sources of the changes, and their future  
659 implications.

660

### 661 **5.1 Sources of change**

662 The existence of mean rates of change in ice and air over our 15-year period imply an imbalance  
663 in the other terms of (9) and (10) during this time. We consider the ability of each of these  
664 terms to cause the imbalance and therefore the ice and air losses. Whether the budget was ever  
665 balanced in the past, with the observed imbalance then implying that changes have occurred,  
666 is a separate question that we cannot answer.

667

668 We start with sources and sinks. Above-balance basal melting will cause ice loss but not air  
669 loss, and can easily account for our ice loss signal. Any melting greater than a few centimetres  
670 per year can cause an imbalance (Figure 7), and observations and models easily support the  
671 rates of  $\sim 0.26$  m/y needed to explain the ice loss (Holland et al., 2009; Mueller et al., 2012;  
672 Nicholls et al., 2012). Above-balance surface melting and refreezing or dry compaction  
673 (through atmospheric warming) will cause only air loss, and it is again easy for these processes  
674 to account for the air loss signal observed here. Below-balance surface accumulation will cause  
675 air and ice loss at a ratio of 2:1—1:1 if snow is initially deposited at a density of 350—450 kg  
676  $\text{m}^{-3}$  (Kuipers Munneke et al., 2012b) and compensating compaction changes are ignored.

677 Below-balance accumulation of approximately half of the modelled value (Figure 7) would be  
678 required to solely explain our ice loss, and the fact that our ice loss is an order of magnitude  
679 larger than the air loss suggests that below-balance accumulation alone cannot account for both.  
680 A small below-balance accumulation could, however, explain the air loss. Since the total input  
681 of air into the firn is 0.5—1 m/y, relatively small anomalies in surface melting, dry compaction,  
682 or accumulation are required to yield the observed 0.04 m/y air loss.

683

684 We now turn to dynamic mechanisms. Above-balance ice flow advection will affect air and ice  
685 thicknesses in proportion to their relative gradients along-flow. According to the results of  
686 Holland et al. (2011), increased advection would enhance the flow of thicker ice with less firn  
687 air across the survey line. The air thickness increases along-flow by approximately 1 m for  
688 every 10 m decrease in along-flow ice thickness. Above-balance advection would therefore  
689 cause air loss, but accompanied by ice gain approximately ten times faster, which entirely  
690 contradicts our observed signals. Above-balance ice flow divergence will cause air and ice  
691 losses in proportion to their relative thicknesses, approximately 1:30 for characteristic ice and  
692 air thicknesses of 10 m and 300 m. The largest velocity change in the literature is an  
693 acceleration of 80 m/y between 2000 and 2006 surveys of northern LCIS (Haug et al., 2010;  
694 Khazendar et al., 2011). If this acceleration caused unbalanced divergence over a length scale  
695 of 100 km, it would cause ice loss of ~0.24 m/y and air loss of ~0.008 m/y. Above-balance  
696 divergence could explain the ice loss, but not the air loss, if maintained at this level and not  
697 accompanied by above-balance advection.

698

699 In summary, the ice loss we observe could be explained by above-balance basal melting and/or  
700 ice divergence, and the air loss could be explained by below-balance accumulation and/or  
701 above-balance surface melting and/or compaction. Our results therefore suggest that at least

702 two different forcings caused the lowering of LCIS during our survey period. Elsewhere around  
703 Antarctica, rapid ice-shelf thinning is thought to be driven by unbalanced ocean melting (e.g.  
704 Shepherd et al., 2004; Holland et al., 2010; Padman et al., 2012; Khazendar et al., 2013), and  
705 our robust evidence of a firn-air loss from LCIS in response to surface processes is the first  
706 direct evidence of an exception to this. The existence of at least two different mechanisms  
707 underlying the change is also consistent with our observation that the ice and air loss signals  
708 have different spatial variation along the survey line.

709

710 The surveys do not encompass all of the known ice-shelf lowering (Figure 1), and it is likely  
711 that the balance of ice and air losses, and their driving mechanisms, varies in different regions  
712 and periods. In particular, our surveys do not capture the rapid lowering in northern LCIS. Ice  
713 divergence may play a part in this, since the known acceleration of LCIS is northward-  
714 intensified (Haug et al., 2010; Khazendar et al., 2011), but there are also good reasons to expect  
715 changes in surface melting to be largest in the north (Holland et al., 2011; Trusel et al., 2013;  
716 Luckman et al., 2014). The pattern of changes in basal melting is unknown.

717

## 718 **5.2 Ice-shelf stability**

719 Our results have important implications for the future stability of LCIS and thus the AP Ice  
720 Sheet. Previous ice-shelf collapses are thought to have been accomplished by surface  
721 meltwater-driven crevassing (van der Veen, 1998; Scambos et al., 2003; van den Broeke, 2005;  
722 Banwell et al., 2013) ~~and/or~~ ice-front retreat past a ‘compressive arch’ in strain rates (Doake et  
723 al., 1998; Kulesa et al., 2014). ~~The northeastern part of LCIS is likely to be least stable, since  
724 it has high surface melting and low firn air [Holland et al., 2011], is showing the most rapid  
725 lowering [Shepherd et al., 2003] and acceleration [Khazendar et al., 2011], is highly crevassed  
726 [McGrath et al., 2012], is slow moving and largely sustained by accumulation, and has a stress~~

727 ~~field conducive to instability [Kulesa et al., 2014].~~ We conceive several interconnected  
728 mechanisms by which LCIS stability could be compromised: 1) ice-front retreat~~s~~ past a  
729 compressive arch; 2) increased surface melting causes firm depletion and meltwater-driven  
730 crevassing; 3) decreased ocean freezing or increased melting depletes marine ice, permitting  
731 the propagation of crevasses; 4) collapse of the Sear Inlet remnant LBIS opens a new ice front  
732 at the northern margin of LCIS; 5) ungrounding from Bawden Ice Rise removes an ice-front  
733 pinning point; 6) ice thinning and acceleration enhances the propagation of crevasses and  
734 weakens shear zones.

735

### 736 **5.2.1 Retreat past compressive arch**

737 Doake et al. (1998) suggested that LBIS was ~~in a stable configuration~~ when the second principal  
738 strain rate was compressive ~~everywhere~~ inshore of a 'compressive arch' near the ice front.  
739 Once this arch was breached by calving, a significant collapse followed. Kulesa et al. (2014)  
740 showed that LCIS has a large region ~~near the ice front~~ in which the second principal stress is  
741 tensile and thus offshore of a compressive arch. Kulesa et al. (2014) also considered the angle  
742 between the flow and first principal stress under the assumption that rifts strike perpendicular  
743 to ~~the flow~~; i, arguing that af the first principal stress ~~is~~ aligned with the flow ~~it will~~  
744 therefore would tend to open rifts, rendering the ice shelf unstable. LCIS has a large region with  
745 near the ice front in which the first principal stress is oriented across-flow, ~~thus~~ stabilising the  
746 ice shelf according to this measure. ~~It is argued that~~ this region is secured by marine ice,  
747 ~~(Kulesa et al., 2014)~~, but there is clearly a risk that calving ~~in this region~~ will remove ice that  
748 ~~both~~ stabilises rifts and shields the compressive arch, leading to ~~a~~ progressive collapse of LCIS.  
749 Worryingly, a rift in the south of LCIS has propagated rapidly beyond a band of marine ice that  
750 has stabilised all such rifts during the observational era (Jansen et al., 2015). Depending upon

751 ~~its evolution, this rift may threaten the LCIS compressive arch within a few years~~(Jansen et al.,  
752 2015).

753 ~~We are unable to assess a timescale for this possibility.~~

754

## 755 **5.2.2 Meltwater-driven crevassing**

756 The ~~final~~ collapse of many AP ice shelves has been linked to the availability of surface  
757 meltwater to enhance the downward propagation of surface crevasses (Scambos et al., 2003;  
758 van den Broeke, 2005; Banwell et al., 2013). There are significant crevasse fields on ~~the surface~~  
759 ~~of~~LCIS, so we hypothesise that ~~future increases in~~ meltwater ponding ~~could contribute to ice~~  
760 ~~shelf collapse is sufficient to drive collapse. Currently, m~~Meltwater ~~is already ponding ponds~~  
761 ~~form~~ in limited areas near the LCIS grounding line (Holland et al., 2011; Luckman et al., 2014),  
762 but these do not pose an imminent risk- ~~of collapseof collapse~~. Before ~~more extensive~~ ponding  
763 can occur it is necessary for the firm to be ~~largely~~ depleted of its air content, since otherwise  
764 meltwater will simply percolate and refreeze. Holland et al. (2011) showed that ~~the nn~~orthern  
765 ~~part of~~LCIS had approximately 10 m of firm air ~~remaining~~ in 1998, while the retreating LBIS  
766 had very little. Our derived air loss of 0.04 m/y would require 250 years to deplete 10 m of air  
767 and threaten LCIS stability. However, the lowest air content and highest lowering are north of  
768 the survey line, and it is likely that surface melting will increase over the coming centuries  
769 (Kuipers Munneke et al., 2014), so this timescale is probably an upper bound.

770

## 771 **5.2.3 Depletion of marine ice**

772 ~~There is plenty of evidence that~~LCIS is stabilised by marine ice (Holland et al., 2009;  
773 Khazendar et al., 2011; Jansen et al., 2013; Kulesa et al., 2014; McGrath et al., 2014), ~~and this~~  
774 ~~implies thatso~~ decreased marine ice deposition or increased melting could allow LCIS to  
775 collapse under its existing ~~stress fieldstrain field~~. ~~The M~~marine ice at the ice front can form a

776 very small fraction of the ice column, implying that the stability of basal crevassing and ~~ice-~~  
777 ~~front~~ calving is controlled by only tens of metres of marine ice (McGrath et al., 2014).  
778 Elsewhere the marine ice can be hundreds of metres thick (Jansen et al., 2013; Kulesa et al.,  
779 2014; McGrath et al., 2014). If our ice loss ~~estimate~~ of 0.3 m/y is caused by unbalanced basal  
780 melting, this suggests a timescale of 170 years to remove the bottom 50 m of ice, destabilising  
781 the ice front, and 500 years to remove ~~the lowest~~ 150 m of ice, destabilising the eastern half of  
782 LCIS. These timescales are extremely uncertain because ~~the the~~ ocean processes driving  
783 melting and freezing are unknown and ~~thus~~ impossible to project. ~~Counter-intuitively,~~  
784 ~~increased ice shelf melting could actually increase the meltwater driven ocean currents and~~  
785 ~~increase their marine ice deposition downstream [Holland et al., 2009].~~ If marine ice deposition  
786 were to cease altogether, it would take 400—500 years to remove the existing marine ice from  
787 LCIS ~~solely~~ by lateral ice advection and iceberg calving.

788

#### 789 5.2.4 Collapse of ~~Sear Inlet~~ remnant LBIS

790 Albrecht and Levermann (2014) propose that ~~an ice shelf~~ the collapse ~~of any ice shelf~~ can  
791 destabilise neighbouring ice shelves by changing their stress regime. ~~For~~ ~~In the context of~~  
792 LCIS, this translates into the risk that ~~a the collapse of LBIS~~ collapse could removes buttressing  
793 by ungrounding ice along ~~across~~ Jason Peninsula. When the majority of LBIS collapsed in 2002,  
794 a remnant ice shelf was left immediately adjacent to LCIS (Figure 9a). ~~–Sear Inlet, the last~~  
795 ~~remaining part of LBIS, This ice is~~ presumably accelerating and apparently weakening  
796 (Khazendar et al., in press) ~~at risk of disintegration~~, so we ~~assess~~ consider the impact upon LCIS  
797 ~~of this possibility of its potential removal on LCIS~~. Jason Peninsula anchors a large area of  
798 stagnant ice that is a significant stabilising influence on both LCIS and ~~Sear Inlet~~ the remnant  
799 LBIS (Figure 9a). The ice ~~dividing between~~ LCIS and ~~Sear Inlet~~ LBIS, Phillipi Rise, is poorly  
800 surveyed but appears to be well-grounded at present, ~~with ice~~ 150 m above floatation

801 (calculated using 5 m firm air from Holland et al. (2011), EIGEN-6C geoid, and mean dynamic  
802 ocean topography of -1 m; Figure 9b). However, the ice base is hundreds of metres below sea  
803 level ~~in places~~ (Figure 9c), so if the remnant LBIS were to collapse it is possible there is  
804 certainly the possibility that subsequent ice thinning could unground Phillipi Rise, removing  
805 buttressing from LCIS and opening a new oceanographic pathway ~~through Jason Peninsula.~~  
806 The timescale for such a possibility is impossible to predict and, ~~However,~~ given the stagnant  
807 nature of this ice, it is unclear to what extent this would influence LCIS stability.

808

### 809 5.2.5 Ungrounding from Bawden Ice Rise

810 ~~Of far greater concern is the stability of Bawden Ice Rise.~~ An ungrounding from Bawden Ice  
811 Rise would prompt significant acceleration of ~~the ice shelf~~ LCIS (Borstad et al., 2013) and re-  
812 organisation of its strain ~~rate~~ field, probably destabilising the ice front (Kulesa et al., 2014).  
813 Bawden ~~The ice rise~~ is only a few kilometres across, but has a significant ~~noticeable~~ effect upon  
814 the flow and structure of the ice shelf (Figure 10a). Three radar survey lines show that  
815 Bawden ~~the ice rise~~ is very lightly grounded in the north, but approximately 40 m above  
816 floatation at its summit in the south (Figure 10b), where the ice base is about 150 m below sea  
817 level (Figure 10c). (Height above floatation is calculated using a 10 m firm air content derived  
818 from nearby surveyed floating ice and finding elevation relative to sea level using nearby  
819 surveyed open water.) Our ice loss estimate of 0.3 m/y would take 130 years to unground  
820 Bawden ~~the ice rise~~ entirely, but this timescale is subject to great uncertainty, including the ice  
821 loss estimate itself, its applicability to this region, and ~~its~~ the projection ~~of this rate~~ into the  
822 future. It is almost certainly an upper bound because lowering is rapid in the region (Figure 1)  
823 and Bawden would cease to provide a significant stabilising influence, and may even  
824 destabilise the ice front, long before the ice ~~actually~~ ungrounds through thinning. For example,  
825 Doake and Vaughan (1991) showed that ice rises ~~destabilised Wordie Ice Shelf by~~ acting as

826 an ‘indenting wedge’ during the retreat of Wordie Ice Shelf~~.its ice front~~. A large calving  
827 occurred south of Bawden between late December 2004 and early January 2005 and the  
828 ongoing thinning (Paolo et al., in press) and acceleration (Khazendar et al., 2011) in in the  
829 region~~this region~~ might even could indicate that ungrounding from Bawden is ~~already~~  
830 underway.

831

### 832 **5.2.6 Crevassing weakens shear zones**

833 Whatever its source, ~~the ongoing~~ thinning and acceleration of LCIS could ultimately cause its  
834 demise by weakening the structural integrity of the ice shelf. LAIS and LBIS both accelerated  
835 before collapsing (Bindschadler et al., 1994; Rignot et al., 2004), and LBIS apparently  
836 collapsed after weakening of the shear zones between ice flow units (Khazendar et al., 2007;  
837 Vieli et al., 2007; Glasser and Scambos, 2008). The shear zones in ~~the north of~~ LCIS are ~~slower-~~  
838 ~~moving and not so less~~ strongly sheared (Khazendar et al., 2011) and hence more stable, but the  
839 ice is already quite damaged (Jansen et al., 2010; McGrath et al., 2012; Borstad et al., 2013).  
840 The uncertainties in this interaction are large and we are unable to assess a timescale for this  
841 risk.

842

## 843 **6. Conclusions**

844 We analyse eight repeated radar surveys between 1998 and 2012 along a nearly meridional line  
845 that traverses the centre of Larsen C Ice Shelf (LCIS), applying a novel method to derive the  
846 separate ice and air losses along this line contributing to the known lowering of the ice shelf.  
847 The uncertainties are considerable, but our primary estimate is that the lowering ( $0.066 \pm 0.017$   
848 m/y, or  $0.99 \pm 0.26$  m) is caused by both ice loss ( $0.28 \pm 0.18$  m/y, or  $4.2 \pm 2.7$  m) and firn air loss  
849 ( $0.037 \pm 0.026$  m/y, or  $0.56 \pm 0.39$  m). Though their effect on the surface lowering is  
850 approximately equal because the ice is floating, ice loss is an order of magnitude larger than

851 air loss and so the results suggest that ice loss is the dominant change affecting LCIS. The  
852 derivation of these values allows us to speculate upon the possible sources of the changes, and  
853 their future implications.

854

855 The ice loss we observe could be explained by above-balance basal melting and/or ice  
856 divergence, and the air loss could be explained by below-balance accumulation and/or above-  
857 balance surface melting and/or compaction. We conclude that at least two different forcings  
858 caused the lowering of LCIS during our survey period. The surveys do not sample the most  
859 rapid ice-shelf lowering in northern LCIS and it is likely that the balance of ice and air losses,  
860 and their driving mechanisms, varies for different regions and periods.

861

862 We conceive several interconnected mechanisms by which LCIS stability could be  
863 compromised, ~~and our ice and air loss rates suggest typical timescales for LCIS collapse of a~~  
864 ~~few centuries~~. The two mechanisms that offer the earliest possibility of collapse are a flow  
865 perturbation arising from the ungrounding of LCIS from Bawden Ice Rise, and ice-front retreat  
866 past a ‘compressive arch’ in strain rates, Ice lowering is now focussed around Bawden Ice  
867 Rise (Paolo et al., in press), and the anomalous propagation of a rift in the south of LCIS may  
868 threaten the compressive arch (Jansen et al., 2015), ~~suggesting that the stability of Bawden Ice~~  
869 ~~Rise and calving from the ice front~~ either mechanism could pose an imminent risk and both  
870 should be monitored closely.

871

## 872 **Acknowledgements**

873

874 We gratefully acknowledge the vital contribution of many dedicated field-workers and support  
875 staff in enabling the radar and satellite campaigns underpinning this study. The imagery in

876 Figure 10 was provided by the Polar Geospatial ~~Centre~~Center at the University of Minnesota  
877 under NSF OPP agreement ANT-1043681. Laurie Padman is gratefully acknowledged for  
878 providing the satellite radar altimetry data and much useful advice.

879

## 880 **References**

881 Albrecht, T., and Levermann, A.: Spontaneous ice-front retreat caused by disintegration of  
882 adjacent ice shelf in Antarctica, *Earth and Planetary Science Letters*, 393, 26-30, DOI  
883 10.1016/j.epsl.2014.02.034, 2014.

884 Arcone, S. A.: Airborne-radar stratigraphy and electrical structure of temperate firn: Bagley  
885 Ice Field, Alaska, USA, *Journal of Glaciology*, 48, 317-334, Doi  
886 10.3189/172756502781831412, 2002.

887 Banwell, A. F., MacAyeal, D., and Sergienko, O. V.: Breakup of the Larsen B Ice Shelf  
888 triggered by chain reaction drainage of supraglacial lakes, *Geophysical Research Letters*,  
889 40, 5872-5876, 10.1002/2013GL057694, 2013.

890 Barrand, N. E., Vaughan, D. G., Steiner, N., Tedesco, M., Munneke, P. K., van den Broeke,  
891 M. R., and Hosking, J. S.: Trends in Antarctic Peninsula surface melting conditions from  
892 observations and regional climate modeling, *Journal of Geophysical Research-Earth  
893 Surface*, 118, 315-330, 10.1029/2012jf002559, 2013.

894 Bathmann, U., Smetacek, V., de Baar, H., Fahrbach, E., and Krause, G.: The expeditions  
895 ANTARKTIS X/6-8 of the research vessel "POLARSTERN" in 1992/93, Alfred-  
896 Wegener-Institut, Bremerhaven, Germany, 236 pp, 1994.

897 Berthier, E., Scambos, T. A., and Shuman, C. A.: Mass loss of Larsen B tributary glaciers  
898 (Antarctic Peninsula) unabated since 2002, *Geophysical Research Letters*, 39, L13501,  
899 10.1029/2012gl051755, 2012.

900 Bindschadler, R. A., Fahnestock, M. A., Skvarca, P., and Scambos, T. A.: Surface-Velocity  
901 Field of the Northern Larsen Ice Shelf, Antarctica, *Annals of Glaciology*, Vol 20, 1994,  
902 20, 319-326, Doi 10.3189/172756494794587294, 1994.

903 Borstad, C. P., Rignot, E., Mouginot, J., and Schodlok, M. P.: Creep deformation and  
904 buttressing capacity of damaged ice shelves: theory and application to Larsen C ice shelf,  
905 *The Cryosphere*, 7, 1931-1947, 10.5194/tc-7-1931-2013, 2013.

906 Brisbourne, A. M., Smith, A. M., King, E. C., Nicholls, K. W., Holland, P. R., and Makinson,  
907 K.: Seabed topography beneath Larsen C Ice Shelf from seismic soundings, *The*  
908 *Cryosphere*, 8, 1-13, 10.5194/tc-8-1-2014, 2014.

909 Cook, A. J., and Vaughan, D. G.: Overview of areal changes of the ice shelves on the Antarctic  
910 Peninsula over the past 50 years, *The Cryosphere*, 4, 77-98, 10.5194/Tc-4-77-2010,  
911 2010.

912 Doake, C. S. M., and Vaughan, D. G.: Rapid Disintegration of the Wordie Ice Shelf in Response  
913 to Atmospheric Warming, *Nature*, 350, 328-330, 10.1038/350328a0, 1991.

914 Doake, C. S. M., Corr, H. F. J., Rott, H., Skvarca, P., and Young, N. W.: Breakup and  
915 conditions for stability of the northern Larsen Ice Shelf, Antarctica, *Nature*, 391, 778-  
916 780, Doi 10.1038/35832, 1998.

917 Domack, E., Duran, D., Leventer, A., Ishman, S., Doane, S., McCallum, S., Amblas, D., Ring,  
918 J., Gilbert, R., and Prentice, M.: Stability of the Larsen B ice shelf on the Antarctic  
919 Peninsula during the Holocene epoch, *Nature*, 436, 681-685, 10.1038/Nature03908,  
920 2005.

921 Dutrieux, P., Vaughan, D. G., Corr, H. F. J., Jenkins, A., Holland, P. R., Joughin, I., and  
922 Fleming, A. H.: Pine Island Glacier ice shelf melt distributed at kilometre scales, *The*  
923 *Cryosphere Discussions*, 2013.

924 Fricker, H. A., and Padman, L.: Thirty years of elevation change on Antarctic Peninsula ice  
925 shelves from multimission satellite radar altimetry, *Journal of Geophysical Research-*  
926 *Oceans*, 117, C02026, 10.1029/2011jc007126, 2012.

927 Glasser, N. F., and Scambos, T. A.: A structural glaciological analysis of the 2002 Larsen B  
928 ice-shelf collapse, *Journal of Glaciology*, 54, 3-16, Doi 10.3189/002214308784409017,  
929 2008.

930 Griggs, J. A., and Bamber, J. L.: Ice shelf thickness over Larsen C, Antarctica, derived from  
931 satellite altimetry, *Geophysical Research Letters*, 36, L19501, 10.1029/2009gl039527,  
932 2009.

933 Haug, T., Kaab, A., and Skvarca, P.: Monitoring ice shelf velocities from repeat MODIS and  
934 Landsat data - a method study on the Larsen C ice shelf, Antarctic Peninsula, and 10  
935 other ice shelves around Antarctica, *The Cryosphere*, 4, 161-178, 10.5194/tc-4-161-  
936 2010, 2010.

937 Hellmer, H. H., Huhn, O., Gomis, D., and Timmermann, R.: On the freshening of the  
938 northwestern Weddell Sea continental shelf, *Ocean Science*, 7, 305-316, 10.5194/os-7-  
939 305-2011, 2011.

940 Holland, P. R., Corr, H. F. J., Vaughan, D. G., Jenkins, A., and Skvarca, P.: Marine ice in  
941 Larsen Ice Shelf, *Geophysical Research Letters*, 36, L11604, 10.1029/2009gl038162,  
942 2009.

943 Holland, P. R., Jenkins, A., and Holland, D. M.: Ice and ocean processes in the Bellingshausen  
944 Sea, Antarctica, *Journal of Geophysical Research-Oceans*, 115, C05020,  
945 10.1029/2008jc005219, 2010.

946 Holland, P. R., Corr, H. F. J., Pritchard, H. D., Vaughan, D. G., Arthern, R. J., Jenkins, A., and  
947 Tedesco, M.: The air content of Larsen Ice Shelf, *Geophysical Research Letters*, 38,  
948 L10503, 10.1029/2011gl047245, 2011.

949 Jansen, D., Kulessa, B., Sammonds, P. R., Luckman, A., King, E. C., and Glasser, N. F.:  
950 Present stability of the Larsen C ice shelf, Antarctic Peninsula, *Journal of Glaciology*,  
951 56, 593-600, Doi 10.3189/002214310793146223, 2010.

952 Jansen, D., Luckman, A., Kulessa, B., Holland, P. R., and King, E. C.: Marine ice formation in  
953 a suture zone on the Larsen C Ice Shelf and its influence on ice shelf dynamics, *Journal*  
954 *of Geophysical Research-Earth Surface*, 118, 1628-1640, Doi 10.1002/Jgrf.20120, 2013.

955 Jansen, D., Luckman, A. J., Cook, A., Bevan, S., Kulessa, B., Hubbard, B., and Holland, P. R.:  
956 Newly developing rift in Larsen C Ice Shelf presents significant risk to stability, *The*  
957 *Cryosphere Discussions*, 9, 861-872, 10.5194/tcd-9-861-2015, 2015.

958 Jullion, L., Garabato, A. C. N., Meredith, M. P., Holland, P. R., Courtois, P., and King, B. A.:  
959 Decadal Freshening of the Antarctic Bottom Water Exported from the Weddell Sea,  
960 *Journal of Climate*, 26, 8111-8125, 10.1175/Jcli-D-12-00765.1, 2013.

961 Khazendar, A., Rignot, E., and Larour, E.: Larsen B Ice Shelf rheology preceding its  
962 disintegration inferred by a control method, *Geophysical Research Letters*, 34, L19503,  
963 10.1029/2007gl030980, 2007.

964 Khazendar, A., Rignot, E., and Larour, E.: Acceleration and spatial rheology of Larsen C Ice  
965 Shelf, Antarctic Peninsula, *Geophysical Research Letters*, 38, L09502,  
966 10.1029/2011gl046775, 2011.

967 Khazendar, A., Schodlok, M. P., Fenty, I., Ligtenberg, S. R. M., Rignot, E., and van den  
968 Broeke, M. R.: Observed thinning of Totten Glacier is linked to coastal polynya  
969 variability, *Nature Communications*, 4, 2857, 10.1038/Ncomms3857, 2013.

970 Khazendar, A., Borstad, C. P., Scheuchl, B., Rignot, E., and Seroussi, H.: The evolving  
971 instability of the remnant Larsen B Ice Shelf and its tributary glaciers, *Earth and*  
972 *Planetary Science Letters*, 10.1016/j.epsl.2015.03.014, in press.

973 King, M. A., and Padman, L.: Accuracy assessment of ocean tide models around Antarctica,  
974 Geophysical Research Letters, 32, L23608, 10.1029/2005gl023901, 2005.

975 Kuipers Munneke, P., Picard, G., van den Broeke, M. R., Lenaerts, J. T. M., and van Meijgaard,  
976 E.: Insignificant change in Antarctic snowmelt volume since 1979, Geophysical  
977 Research Letters, 39, L01501, 10.1029/2011gl050207, 2012a.

978 Kuipers Munneke, P., van den Broeke, M. R., King, J. C., Gray, T., and Reijmer, C. H.: Near-  
979 surface climate and surface energy budget of Larsen C ice shelf, Antarctic Peninsula, The  
980 Cryosphere, 6, 353-363, 10.5194/tc-6-353-2012, 2012b.

981 Kuipers Munneke, P., Ligtenberg, S. R. M., van den Broeke, M. R., and Vaughan, D. G.: Firn  
982 air depletion as a precursor of Antarctic ice-shelf collapse, Journal of Glaciology, 60,  
983 205-214, Doi 10.3189/2014jog13j183, 2014.

984 Kulesa, B., Jansen, D., Luckman, A. J., King, E. C., and Sammonds, P. R.: Marine ice  
985 regulates the future stability of a large Antarctic ice shelf, Nature Communications, 5,  
986 3707, 10.1038/Ncomms4707, 2014.

987 Lenaerts, J. T. M., van den Broeke, M. R., van de Berg, W. J., van Meijgaard, E., and Munneke,  
988 P. K.: A new, high-resolution surface mass balance map of Antarctica (1979-2010) based  
989 on regional atmospheric climate modeling, Geophysical Research Letters, 39, L04501,  
990 10.1029/2011gl050713, 2012.

991 Luckman, A., Elvidge, A., Jansen, D., Kulesa, B., Munneke, P. K., King, J. C., and Barrand,  
992 N. E.: Surface melt and ponding on Larsen C Ice Shelf and the impact of foehn winds,  
993 Antarctic Science, 26, 625-635, 2014.

994 Marshall, G. J., Orr, A., van Lipzig, N. P. M., and King, J. C.: The impact of a changing  
995 Southern Hemisphere Annular Mode on Antarctic Peninsula summer temperatures,  
996 Journal of Climate, 19, 5388-5404, 10.1175/Jcli3844.1, 2006.

997 McGrath, D., Steffen, K., Scambos, T., Rajaram, H., Casassa, G., and Lagos, J. L. R.: Basal  
998 crevasses and associated surface crevassing on the Larsen C ice shelf, Antarctica, and  
999 their role in ice-shelf instability, *Annals of Glaciology*, 53, 10-18,  
1000 10.3189/2012aog60a005, 2012.

1001 McGrath, D., Steffen, K., Holland, P. R., Scambos, T., Rajaram, H., Abdalati, W., and Rignot,  
1002 E.: The structure and effect of suture zones in the Larsen C Ice Shelf, Antarctica, *Journal*  
1003 *of Geophysical Research-Earth Surface*, 119, 588-602, 10.1002/2013jf002935, 2014.

1004 Morris, E. M., and Vaughan, D. G.: Spatial and temporal variation of surface temperature on  
1005 the Antarctic Peninsula and the limit of viability of ice shelves, *Antarctic Peninsula*  
1006 *Climate Variability: Historical and Paleoenvironmental Perspectives*, 79, 61-68, 2003.

1007 Mueller, R. D., Padman, L., Dinniman, M. S., Erofeeva, S. Y., Fricker, H. A., and King, M.  
1008 A.: Impact of tide-topography interactions on basal melting of Larsen C Ice Shelf,  
1009 Antarctica, *Journal of Geophysical Research-Oceans*, 117, C05005,  
1010 10.1029/2011jc007263, 2012.

1011 Nicholls, K. W., Pudsey, C. J., and Morris, P.: Summertime water masses off the northern  
1012 Larsen C Ice Shelf, Antarctica, *Geophysical Research Letters*, 31, L09309,  
1013 10.1029/2004gl019924, 2004.

1014 Nicholls, K. W., Makinson, K., and Venables, E. J.: Ocean circulation beneath Larsen C Ice  
1015 Shelf, Antarctica from in situ observations, *Geophysical Research Letters*, 39, L19608,  
1016 10.1029/2012gl053187, 2012.

1017 Padman, L., King, M., Goring, D., Corr, H., and Coleman, R.: Ice-shelf elevation changes due  
1018 to atmospheric pressure variations, *Journal of Glaciology*, 49, 521-526, Doi  
1019 10.3189/172756503781830386, 2003.

1020 Padman, L., Costa, D. P., Dinniman, M. S., Fricker, H. A., Goebel, M. E., Huckstadt, L. A.,  
1021 Humbert, A., Joughin, I., Lenaerts, J. T. M., Ligtenberg, S. R. M., Scambos, T., and van

1022 den Broeke, M. R.: Oceanic controls on the mass balance of Wilkins Ice Shelf,  
1023 Antarctica, *Journal of Geophysical Research-Oceans*, 117, C01010,  
1024 10.1029/2011jc007301, 2012.

1025 Paolo, F. S., Fricker, H. A., and Padman, L.: Volume loss from Antarctic ice shelves is  
1026 accelerating, *Science*, in press.

1027 Pritchard, H. D., Ligtenberg, S. R. M., Fricker, H. A., Vaughan, D. G., van den Broeke, M. R.,  
1028 and Padman, L.: Antarctic ice-sheet loss driven by basal melting of ice shelves, *Nature*,  
1029 484, 502-505, 10.1038/Nature10968, 2012.

1030 Rignot, E., Casassa, G., Gogineni, P., Krabill, W., Rivera, A., and Thomas, R.: Accelerated ice  
1031 discharge from the Antarctic Peninsula following the collapse of Larsen B ice shelf,  
1032 *Geophysical Research Letters*, 31, L18401, 10.1029/2004gl020697, 2004.

1033 Rignot, E., Mouginot, J., and Scheuchl, B.: Ice Flow of the Antarctic Ice Sheet, *Science*, 333,  
1034 1427-1430, 10.1126/science.1208336, 2011.

1035 Rye, C. D., Naveira Garabato, A. C., Holland, P. R., Meredith, M. P., Nurser, A. J. G., Hughes,  
1036 C. W., Coward, A. C., and Webb, D. J.: Evidence of increased glacial melt in Antarctic  
1037 coastal sea level rise, *Nature Geoscience*, 7, 732-735, doi:10.1038/ngeo2230, 2014.

1038 Scambos, T. A., Hulbe, C., and Fahnestock, M.: Climate-induced ice shelf disintegration in the  
1039 Antarctic Peninsula, *Antarctic Peninsula Climate Variability: Historical and*  
1040 *Paleoenvironmental Perspectives*, 79, 79-92, 2003.

1041 Scambos, T. A., Haran, T. M., Fahnestock, M. A., Painter, T. H., and Bohlander, J.: MODIS-  
1042 based Mosaic of Antarctica (MOA) data sets: Continent-wide surface morphology and  
1043 snow grain size, *Remote Sensing of Environment*, 111, 242-257, DOI  
1044 10.1016/j.rse.2006.12.020, 2007.

1045 Shepherd, A., Wingham, D., Payne, T., and Skvarca, P.: Larsen Ice Shelf has progressively  
1046 thinned, *Science*, 302, 856-859, 10.1126/science.1089768, 2003.

1047 Shepherd, A., Wingham, D., and Rignot, E.: Warm ocean is eroding West Antarctic Ice Sheet,  
1048 Geophysical Research Letters, 31, L23402, 10.1029/2004gl021106, 2004.

1049 Shepherd, A., Wingham, D., Wallis, D., Giles, K., Laxon, S., and Sundal, A. V.: Recent loss  
1050 of floating ice and the consequent sea level contribution, Geophysical Research Letters,  
1051 37, L13503, 10.1029/2010gl042496, 2010.

1052 Shepherd, A., Ivins, E. R., Geruo, A., Barletta, V. R., Bentley, M. J., Bettadpur, S., Briggs, K.  
1053 H., Bromwich, D. H., Forsberg, R., Galin, N., Horwath, M., Jacobs, S., Joughin, I., King,  
1054 M. A., Lenaerts, J. T. M., Li, J. L., Ligtenberg, S. R. M., Luckman, A., Luthcke, S. B.,  
1055 McMillan, M., Meister, R., Milne, G., Mouginot, J., Muir, A., Nicolas, J. P., Paden, J.,  
1056 Payne, A. J., Pritchard, H., Rignot, E., Rott, H., Sorensen, L. S., Scambos, T. A.,  
1057 Scheuchl, B., Schrama, E. J. O., Smith, B., Sundal, A. V., van Angelen, J. H., van de  
1058 Berg, W. J., van den Broeke, M. R., Vaughan, D. G., Velicogna, I., Wahr, J., Whitehouse,  
1059 P. L., Wingham, D. J., Yi, D. H., Young, D., and Zwally, H. J.: A Reconciled Estimate  
1060 of Ice-Sheet Mass Balance, Science, 338, 1183-1189, 10.1126/science.1228102, 2012.

1061 Tedesco, M.: Assessment and development of snowmelt retrieval algorithms over Antarctica  
1062 from K-band spaceborne brightness temperature (1979-2008), Remote Sensing of  
1063 Environment, 113, 979-997, 10.1016/j.rse.2009.01.009, 2009.

1064 Trusel, L. D., Frey, K. E., Das, S. B., Munneke, P. K., and van den Broeke, M. R.: Satellite-  
1065 based estimates of Antarctic surface meltwater fluxes, Geophysical Research Letters, 40,  
1066 6148-6153, 10.1002/2013gl058138, 2013.

1067 Turner, J., Barrand, N. E., Bracegirdle, T. J., Convey, P., Hodgson, D. A., Jarvis, M., Jenkins,  
1068 A., Marshall, G., Meredith, M. P., Roscoe, H., Shanklin, J., French, J., Goosse, H.,  
1069 Guglielmin, M., Gutt, J., Jacobs, S., Kennicutt, M. C., Masson-Delmotte, V., Mayewski,  
1070 P., Navarro, F., Robinson, S., Scambos, T., Sparrow, M., Summerhayes, C., Speer, K.,

1071 and Klepikov, A.: Antarctic climate change and the environment: an update, *Polar*  
1072 *Record*, 50, 237-259, Doi 10.1017/S0032247413000296, 2014.

1073 Valisuo, I., Vihma, T., and King, J. C.: Surface energy budget on Larsen and Wilkins ice  
1074 shelves in the Antarctic Peninsula: results based on reanalyses in 1989--2010, *The*  
1075 *Cryosphere*, 8, 1519-1538, 10.5194/tc-8-1519-2014, 2014.

1076 van den Broeke, M.: Strong surface melting preceded collapse of Antarctic Peninsula ice shelf,  
1077 *Geophysical Research Letters*, 32, L12815, 10.1029/2005gl023247, 2005.

1078 van der Veen, C. J.: Fracture mechanics approach to penetration of surface crevasses on  
1079 glaciers, *Cold Regions Science and Technology*, 27, 31-47, Doi 10.1016/S0165-  
1080 232x(97)00022-0, 1998.

1081 Vieli, A., Payne, A. J., Shepherd, A., and Du, Z.: Causes of pre-collapse changes of the Larsen  
1082 B ice shelf: Numerical modelling and assimilation of satellite observations, *Earth and*  
1083 *Planetary Science Letters*, 259, 297-306, DOI 10.1016/j.epsl.2007.04.050, 2007.

1084 Wingham, D. J., Wallis, D. W., and Shepherd, A.: Spatial and temporal evolution of Pine Island  
1085 Glacier thinning, 1995-2006, *Geophysical Research Letters*, 36, L17501,  
1086 10.1029/2009gl039126, 2009.

1087

1088

Date	Origin	Platform	Ice-Sounding Radar	Ice Elevation
20-Feb-1998	BAS-Argentine	Twin otter	150 MHz <sup>a</sup>	radar altimeter <sup>a</sup>
26-Nov-2002	NASA-CECS	P-3	ICORDS2 140-160 MHz <sup>b</sup>	laser ATM <sup>c</sup>
29-Nov-2004	NASA-CECS	P-3	ACORDS 140-160 MHz <sup>b</sup>	laser ATM <sup>c</sup>
04-Nov-2009	NASA IceBridge	DC-8	MCoRDS 190-200 MHz* <sup>b,d</sup>	laser ATM <sup>c</sup>
19—21-Nov-2009	McGrath	Sledge	25 MHz <sup>e</sup>	GPS <sup>e</sup>
13-Nov-2010	NASA IceBridge	DC-8	MCoRDS 190-200 MHz <sup>b,d</sup>	laser ATM <sup>c</sup>
27-Jan-2011	BAS	Twin otter	150 MHz	radar altimeter
13—14-Dec-2012	Brisbourne	Sledge	50 MHz	GPS

1089 <sup>a</sup> Holland et al. (2009);

1090 <sup>b</sup> <https://data.cresis.ku.edu/#RDS>;

1091 <sup>c</sup> <http://nsidc.org/data/ilatm2>;

1092 <sup>d</sup> <http://nsidc.org/data/irmcr2.html>;

1093 <sup>e</sup> McGrath et al. (2014).

1094 \*Data neglected due to transmit/receive switch problem; see section 2.43.

1095

1096 **Table 1:** Details of the radio-echo sounding and altimeter surveys used in this analysis.

case	elevation (m/y)	TWTT (m ice year <sup>-1</sup> )	ice (m/y)	air (m/y)
Reference	-0.0660	-0.296	-0.274	-0.0367
Using satellite altimetry	-0.0616	-0.296	-0.277	-0.0320
BAS only <sup>a</sup>	-0.0752	-0.264	-0.235	-0.0500
NASA only <sup>b</sup>	-0.0303	<b>0.087</b>	<b>0.110</b>	-0.0421
Without 1998	-0.0311	<b>-0.041</b>	<b>-0.025</b>	-0.0285
Without 2002	-0.0694	-0.389	-0.371	-0.0297
Without 2004	-0.0713	-0.281	-0.256	-0.0439
Without 2009 MG	-0.0654	-0.195	<b>-0.168</b>	-0.0474
Without 2010	-0.0648	-0.351	-0.334	-0.0290
Without 2011	-0.0695	-0.394	-0.377	-0.0292
With 2009 IB TWTT	-0.0660	-0.482	-0.471	<b>-0.0155</b>
With 2012	-0.0670	-0.212	-0.185	-0.0473
Uncertainty (see text)	0.017	0.17	0.18	0.026

1097 <sup>a</sup>All 1998 and 2011 data

1098 <sup>b</sup>All 2002, 2004, 2010 data and elevation for IceBridge 2009.

1099

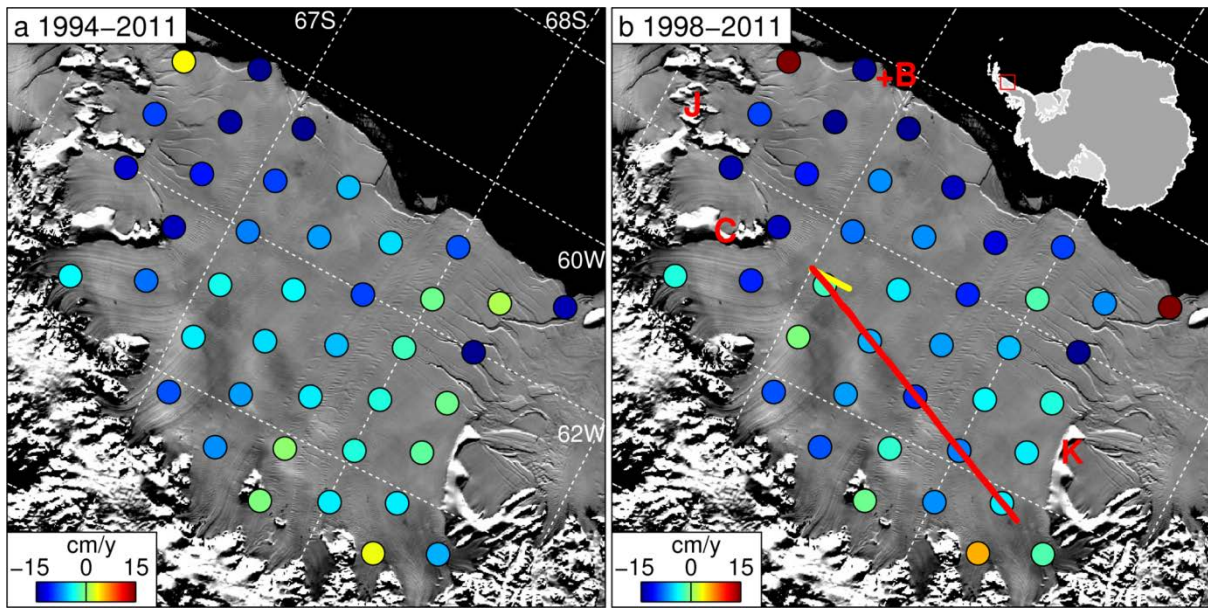
1100 **Table 2:** Elevation and TWTT trends and their derived ice and air trends from calculations  
1101 performed using different combinations of data. TWTT trends are expressed as solid-ice  
1102 thickness equivalent. Trends in bold are smaller than the derived uncertainty (see main text).

survey	elevation differences from 2004 (m)				TWTT differences from 2004 (m ice)			
	count	mean	stddev	stderr	count	mean	stddev	stderr
1998	2213	0.993	1.365	0.029	1382	2.320	7.507	0.202
2002	5092	0.376	1.329	0.019	952	-3.384	9.365	0.304
2004	6097	0	0	0	18385	0	0	0
2009 MG	8731	-0.013	1.726	0.019	4385	-5.441	9.501	0.144
2009 IB*	4779	0.215	1.139	0.017	4444	-11.62	11.91	0.179
2010	4461	-0.088	1.836	0.028	5317	-1.784	9.847	0.135
2011	12126	0.020	1.573	0.014	9190	-1.097	9.802	0.102
2012	303	-0.225	2.401	0.138	187	-0.976	9.651	0.706

\*TWTT data neglected due to transmit/receive switch problem; see section 2.3.

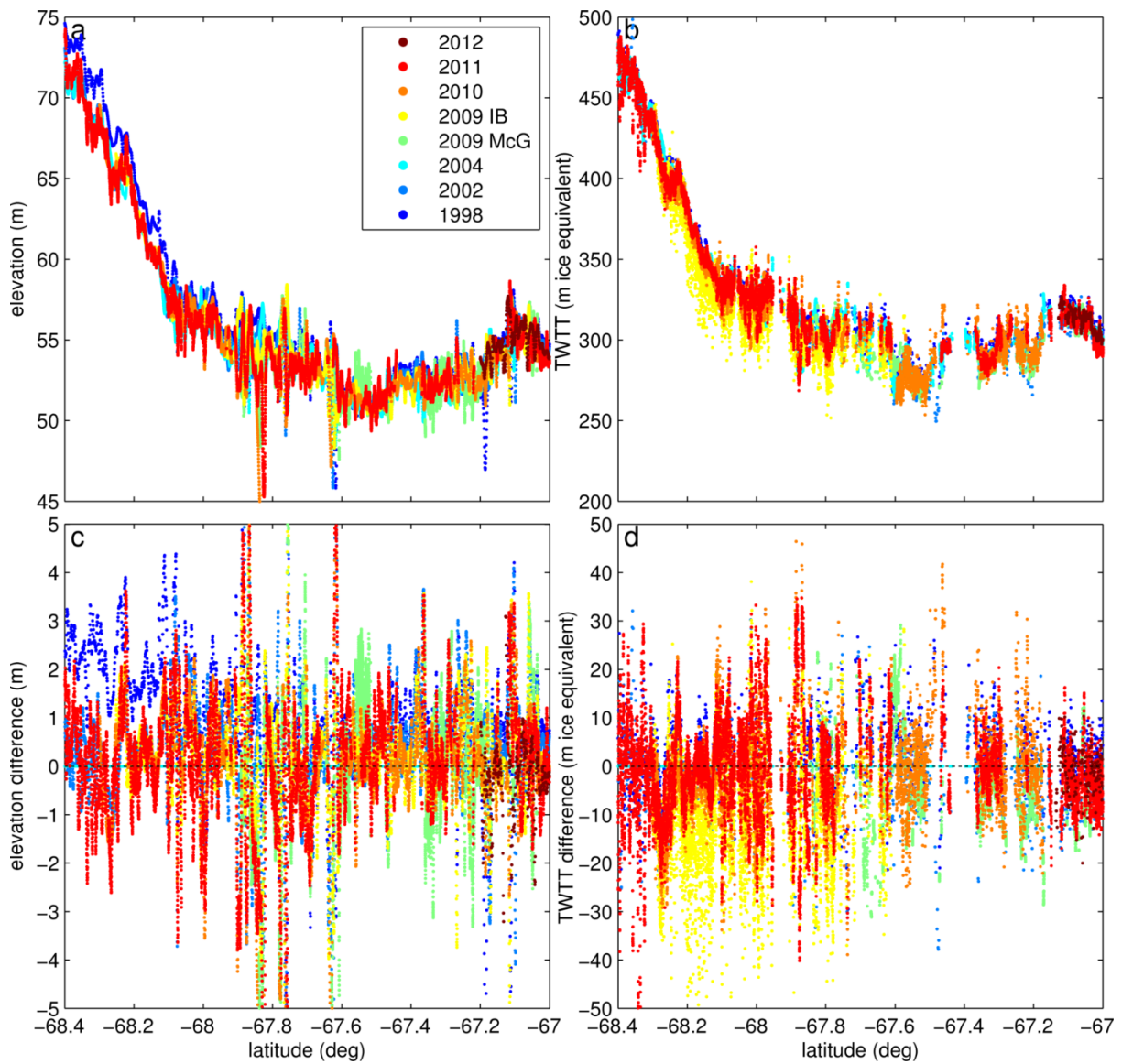
1103  
1104

1105 **Table 3:** Statistics of the differences between all data from each survey and their nearest 2004  
1106 analogue, as shown in Figure 4. TWTT is expressed as solid-ice thickness equivalent.



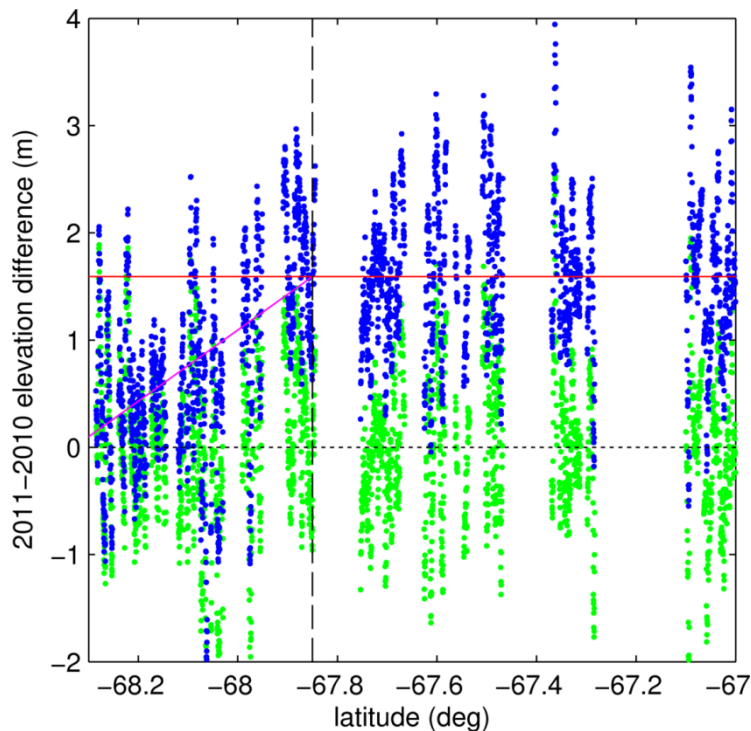
1107

1108 **Figure 1:** MODIS Mosaic of Antarctica imagery of LCIS (Scambos et al., 2007) showing the  
 1109 location of satellite radar altimeter crossovers and estimated surface lowering rates (updated  
 1110 from Fricker and Padman, 2012, as described in section 2.5) for two periods. a) 1994—2011,  
 1111 the full period for which ERS-1/2 and Envisat data are reliable; b) 1998—2011, the period for  
 1112 which we have radar surveys. The main survey line is shown in red, with the 2012 survey  
 1113 shown in yellow. Panel b shows geographical features referred to in the text: B: Bawden Ice  
 1114 Rise; C: Churchill Peninsula; J: Jason Peninsula; K: Kenyon Peninsula.



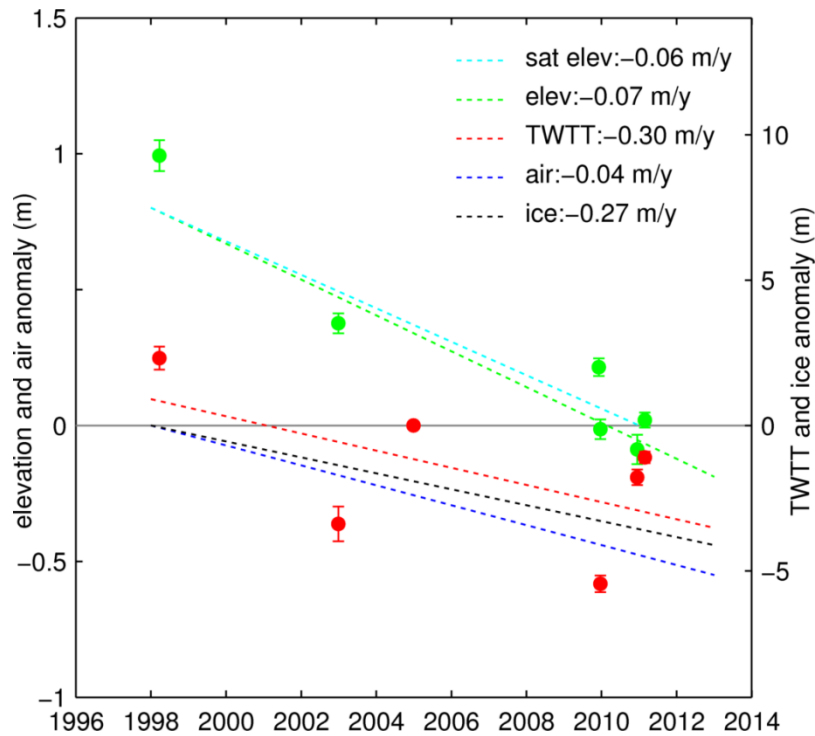
1115

1116 **Figure 2:** Processed data from the eight surveys, from which the air and ice thickness changes  
 1117 are derived. a) Surface elevation relative to WGS84 ellipsoid. b) Radar two-way travel time  
 1118 (TWTT), expressed as an equivalent thickness of solid ice. c) Difference between each  
 1119 elevation observation and nearest 2004 analogue. d) Difference between each TWTT  
 1120 observation and nearest 2004 analogue.



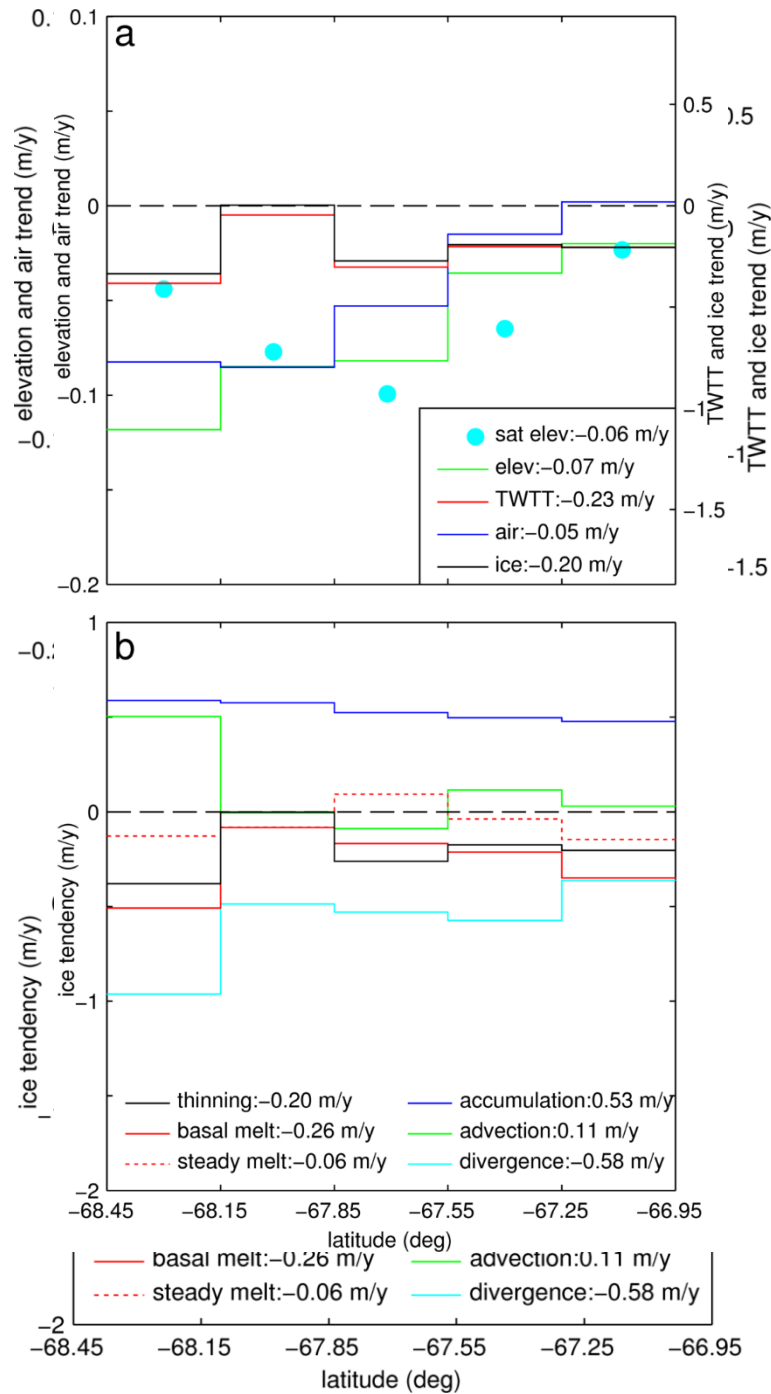
1121

1122 **Figure 3:** ~~Correctionalibration~~ of the elevation data in the 2011 BAS airborne survey. Blue  
 1123 dots ~~show~~indicate the differences ~~between~~ uncorrected elevations derived from BAS radar  
 1124 altimetry elevations on 27 January 2011 ~~and~~and from IceBridge laser altimetry elevations on  
 1125 13 November 2010 (using the sign convention 2011 minus 2010). The 2011 survey data need  
 1126 to be calibrated and also have radar firm penetration removed. Assuming negligible elevation  
 1127 change over the ~~intervening~~ ~10 weeks between surveys, the 2011 data ~~need to be corrected~~are  
 1128 first calibrated by subtracting everywhere an ~~constant~~ offset of 1.59 m (red line; the mean  
 1129 difference from 2010 for all data north of 67.85 °S). After this calibration, South of 67.85 °S,  
 1130 the 2011 data ~~are~~become progressively lower than 2010 south of 67.85 °S, which is attributed  
 1131 to ~~increasing~~ radar penetration of the firn (Holland et al., 2011). In this region we add an  
 1132 additional penetration correction equal to the difference between the red and magenta lines.  
 1133 This ~~penetration~~ correction is also applied to the 1998 BAS radar altimeter data. Green dots  
 1134 show the difference between the ~~corrected 2011~~0 data and the ~~corrected 2010~~1 data.



1135

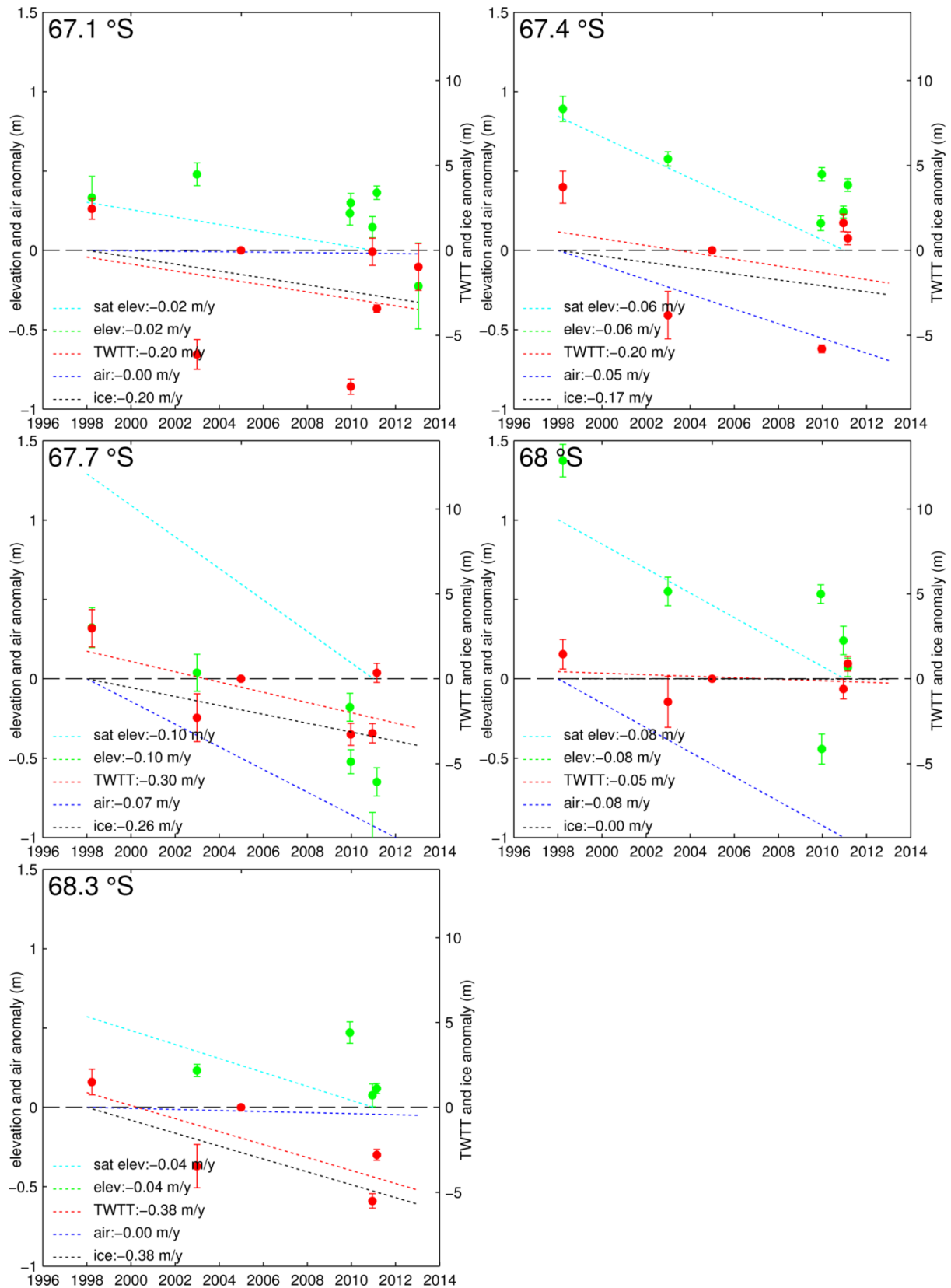
1136 **Figure 4:** Inter-survey differences in elevation, TWTT, ice and air. Mean differences between  
 1137 each survey and 2004 for elevation are shown in green and for radar two-way travel time  
 1138 (TWTT; ice equivalent) in red. Error bars represent 95% confidence intervals of the population  
 1139 of differences from 2004, and dashed lines represent linear trend lines. The 2004 elevation and  
 1140 TWTT are both shown as zero, with zero error. The elevation trend derived from satellite radar  
 1141 altimetry is also shown in cyan. Trends in ice thickness (black) and air thickness (blue)  
 1142 thickness are derived directly from ~~the~~ trends in TWTT and elevation, revealing that LCIS  
 1143 has lost both ice and air over the period surveyed. Elevation and air thickness use the left axis,  
 1144 while TWTT and ice thickness are plotted with absolute values on the right axis and equivalent  
 1145 surface elevation on the left axis. (see section 4).



1146

1147 **Figure 5:** Spatial variation in derived quantities along the survey line within latitude bins  
 1148 centred upon the locations of the satellite cross-over points (see Figure 1b). a) Trends in  
 1149 elevation (green), TWTT (red; ice equivalent), and air (black) and ice (blue) thickness, showing  
 1150 significant ice and air loss. Elevation trends derived from satellite radar altimetry at the  
 1151 crossovers are cyan. Elevation and air thickness use the left axis, while TWTT and ice thickness  
 1152 are plotted with absolute values on the right axis and equivalent surface elevation on the left

1153 axis. b) Spatial variation in ice mass budget. Divergence balances accumulation, and ice  
1154 thinning ~~must be dominated by~~ similar to unbalanced basal melting. Values in the legends  
1155 represent means over all bins.

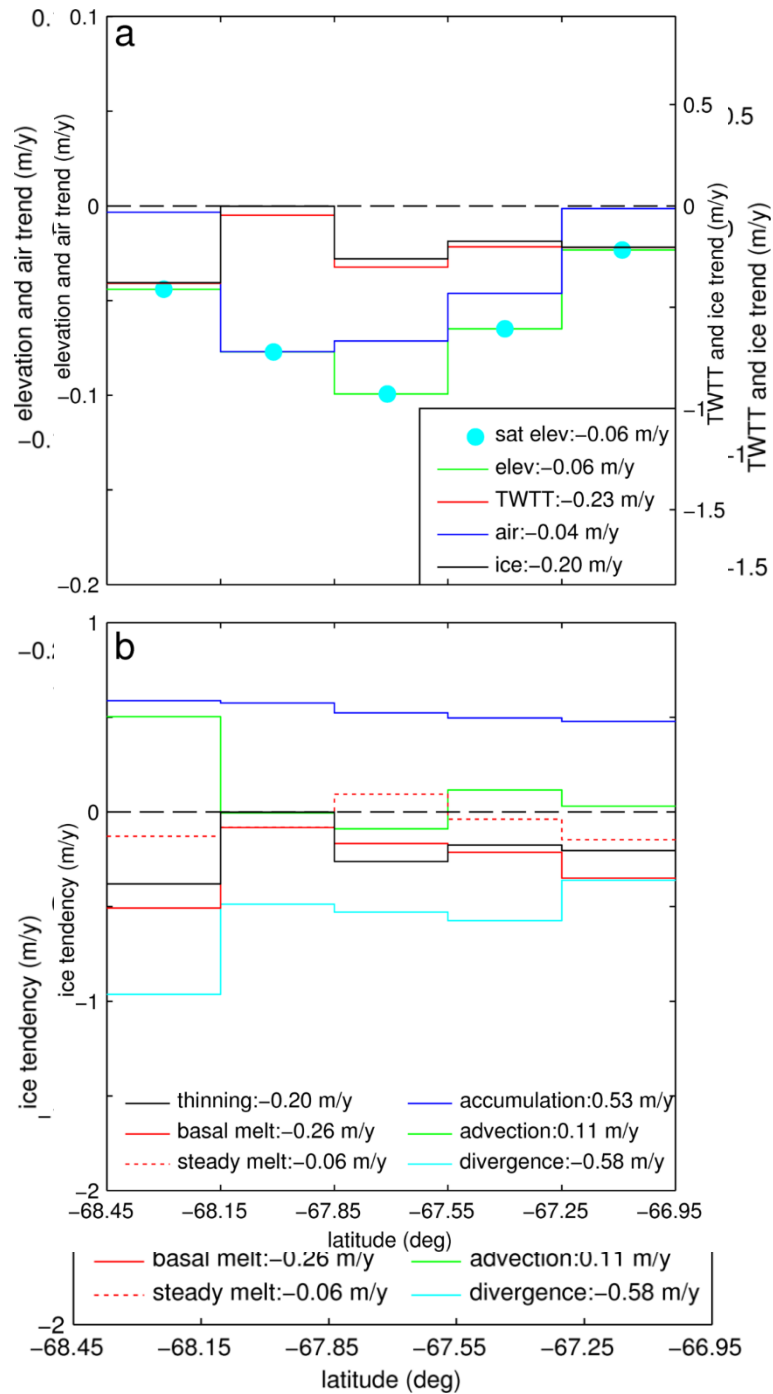


1156

1157 **Figure 6:** Data and trends for the five latitude bins defined by the satellite altimetry crossovers,

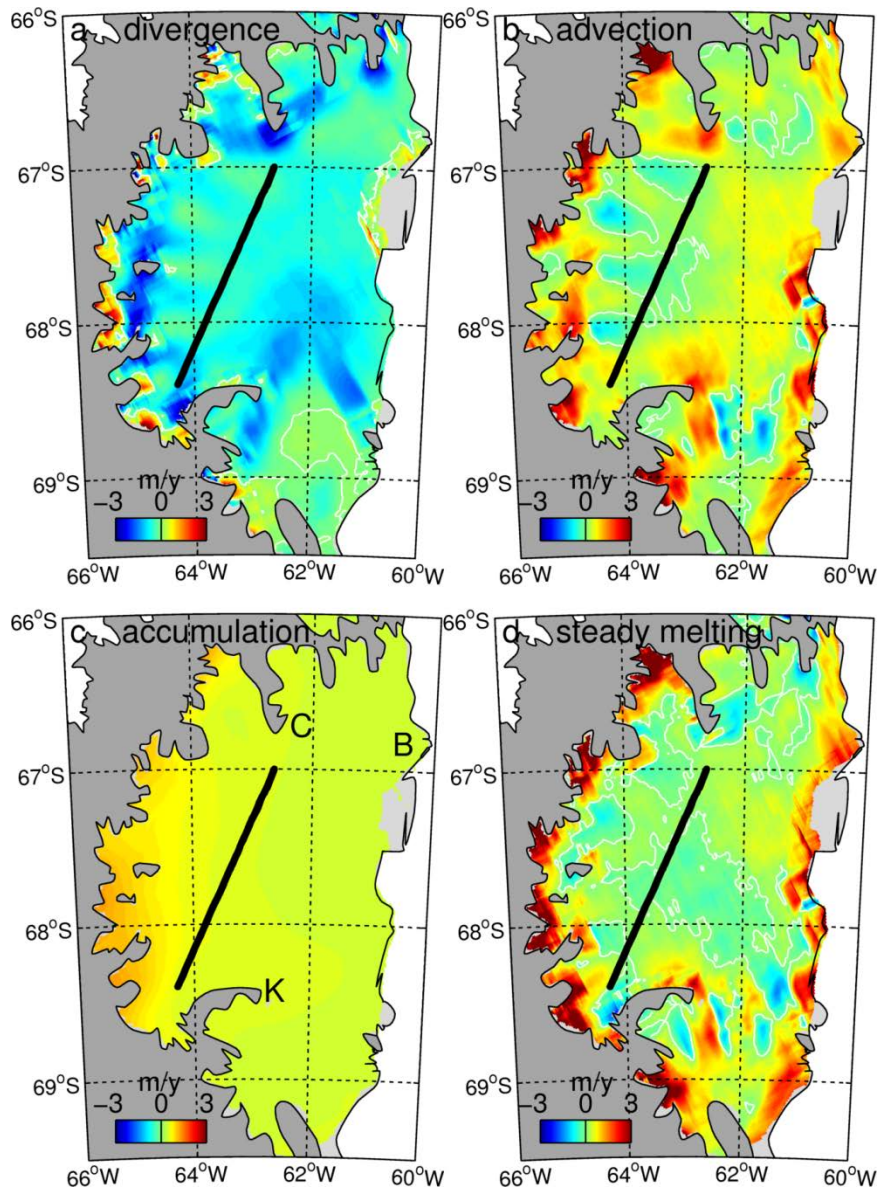
1158 labelled with the latitude of the accompanying crossover. Data points show the mean and 95%

1159 confidence intervals of the differences between each survey and the 2004 baseline for surface  
1160 elevation (green) and TWTT (red, expressed as solid-ice equivalent). The satellite-altimeter  
1161 derived elevation trend for the crossover at the centre of each bin is also shown (cyan).  
1162 Surveyed trends in elevation and TWTT are converted to trends in ice (black) and air (blue)  
1163 thickness. Elevation and air thickness are plotted on the left-hand axis, while TWTT and ice  
1164 thickness are plotted such that the right-hand axis shows absolute values and the left-hand axis  
1165 shows the equivalent surface elevation.



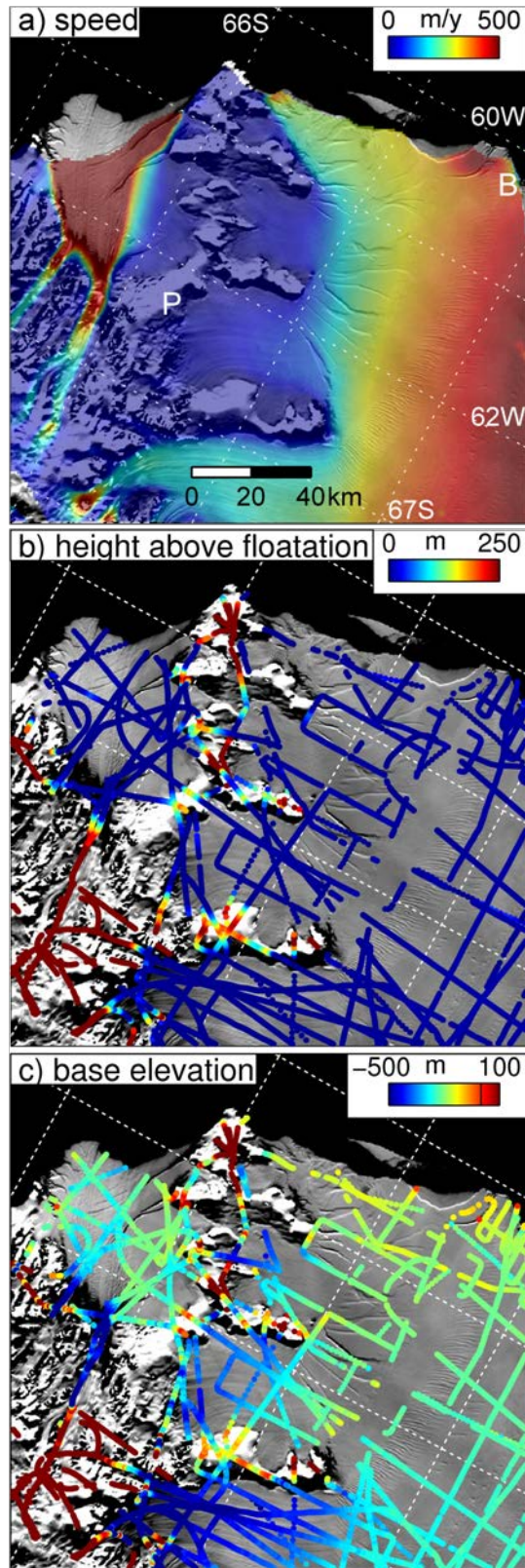
1166

1167 **Figure 7:** Version of Figure 5 in which the binned survey elevation trends are replaced by  
 1168 satellite crossover elevation trends. a) Spatial variation of trends in elevation (green), TWTT  
 1169 (red, ice equivalent), and air (black) and ice (blue) thickness. Satellite crossover trends are  
 1170 cyan. Elevation and air thickness use the left axis, while TWTT and ice thickness are plotted  
 1171 with absolute values on the right axis and equivalent surface elevation on the left axis. b)  
 1172 Meridional variation in ice mass budget.



1173

1174 **Figure 8:** Fields of derived values for the terms in the ice-only mass balance (positive implies  
 1175 melting). a) ice divergence ( $-\nabla \cdot \mathbf{u}$ ); b) ice advection ( $-\mathbf{u} \cdot \nabla I$ ); c) ice surface accumulation;  
 1176 d) derived steady-state basal melting. Panel c shows geographical features referred to in the  
 1177 text: B: Bawden Ice Rise; C: Churchill Peninsula; K: Kenyon Peninsula.



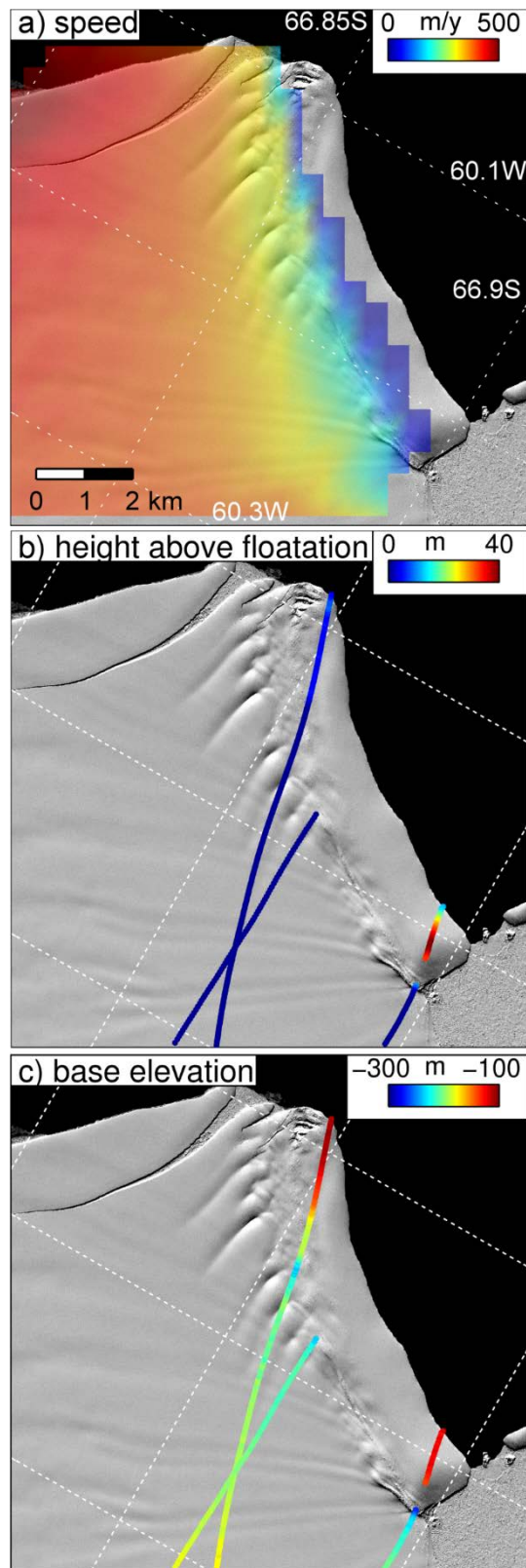
1178

1179 **Figure 9:** Northern LCIS and Jason Peninsula, showing various quantities overlain on MODIS

1180 Mosaic of Antarctica (Scambos et al., 2007). a) ice flow speed (Rignot et al., 2011); b) height

1181 of ice surface above hydrostatic floatation; c) elevation of ice base relative to sea level. Bawden

1182 Ice Rise is labelled B and Phillipi Rise is labelled P.



1183

1184 **Figure 10:** High-resolution WorldView2 satellite imagery of Bawden Ice Rise acquired 15<sup>th</sup>

1185 October 2012 (copyright Digital Globe) with various quantities overlain. a) ice flow speed

1186 (Rignot et al., 2011); b) height of ice surface above hydrostatic floatation; c) elevation of ice  
1187 base relative to sea level.